Politecnico di Milano

School of Industrial Engineering and Information
Department of Aerospace Science and Engineering

Study and calibration of a Hybrid III head model

Advisor: Prof. Paolo Carlo Astori

Coadvisor: Dot. Benedetta Arosio

Tutor UPV: Luis Manuel Sánchez Ruiz

Author: Rodriguez Pastor, Marc

Academic year 2017/2018

Abstract

Dummy testing has become a really important part in the improvement of safety in the means of transport around the world. Anyway, it is an expensive procedure so alternative ways to find the same results have been investigated in order to obtain them with lower costs. For these reasons, computer assisted models (FEM) have exponentially increased in the recent years, being necessary to refine those models to reproduce exactly the behaviour obtained in the experiments.

This thesis tries to achieve this goal, focusing on reproducing the data obtained in two real experiments: head drop and a pendulum's impact on a head. The LS-Dyna models were modified according to the results obtained in a sensitivity analysis of the materials in order to achieve the desired response.

Key words: LS-Dyna, sensitivity analysis, head drop, pendulum's impact,

Contents

Chapter 1

Introduction

In this chapter, a brief description of the particularities of the current work will be discussed. Furthermore, the coefficients that will be used for the comparison between the different experiments and simulations will be explained.

1.1 Problem definition

Crash testing has become recently an important tool for improving the security that passengers of different means of transport enjoy, as it makes feasible to see the possible injuries (head and spine mainly) that a certain accident may cause in a person. Originally, those tests were done with animals and corpses due to their similarity with human body.

Obviously, many sectors in the society were against these activities because of an ethical point of view, so they started to claim for an alternative procedure. Actually, engineers were also looking for another options because they couldn't achieve the repeatability of the results since it was impossible to obtain two corpses exactly equal.

In the last 60 years, the introduction of the Anthropomorphic Test Devices(ATD) mended this issue due to the fact that the dummy allowed to reproduce exactly the conditions held in an experiment, being possible to collect as many data as desired. Finally, Finite-Element computer softwares were implemented for reducing the cost of the tests as well as the time spent for performing them. The main advantage that these softwares offered respect the real experimentation is that different simulations could be set with different paramenters in a short lapse of time. Moreover, the data provided by the HIII physical dummy model could only be found for the specific regions where the instruments were placed. Nevertheless, FE softwares make possible to obtain data from any desired point of the dummy model because the equations that rule the mechanical behaviour are stated everywhere on the model, being possible to look for their numerical solution at any point .

Furthermore, new dummy models have been introduced in the recent years. These FE models have several differences respect to their predecessors so it is absolutely necessary to validate them with real data in order to know if they have improved their results simulating the human being responses.

1.2 Main purpose and objectives of the work

In this work several simulations have been performed in order to see the influence of the "boundary conditions" in the result of the variables of interest (accelerations, forces, moments...). Many data of those parameters have been taken for evaluating the damage that these changes may produce in the human body, calculating them by means of different injury criteria. The key data collected have been:

- Acceleration of head's c.g.: a_x,a_y,a_z
- Forces: F_x,F_y,F_z

- Moments at Occipital Condyle: M_x, M_y

However, data coming from the simulations must be validated in order to improve the software performance and check that the numerical model is correct. For this reason, it was partially recalled an experiment performed at LaST (Politecnico di Milano), the experiment consisted basically in hitting the head of the Hybrid III dummy model with a pendulum from different angles (frontal, upper, lateral). For the present work, it was only used the data coming from the frontal impact to compare it with the results calculated from the simulations for finding out if the models have a similar behaviour respect the real test device .

The results (1) of the experiments performed at LaST were processed using MATLAB. Furthermore, another additional experiment was done for the head drop test. In this case, an isolated head was dropped different heights in order to analyse the accelerations that were originated in the centre of gravity of the head by the hit.

From the simulation's point of view, it was tried to reproduce the experiment performed at the lab with the software (LS-Dyna) using two different ATD dummy model heads: the first model LSTC.H3.103008_V1.0 and an updated version LSTC.NCAC_H3_50TH.130528_BETA. As a first approach, data was properly filtered and compared with the experiment in order to have a first idea of which one had a more realistic behaviour. After that, a sensitivity study was carried out in order to see which parameters of the updated model could lead to a behaviour closer to the reality. These kind of simulations follow a calibration procedure and regulations (4) that set which are the limiting values that the diverse factors involved in the experiment can move between. For this reason, it was performed a sensitivity study of some of those parameters (velocity of pendulum, Young and Bulk modulus of materials...) in order to see how this could affect the value of the parameters.

Additionally, a head drop analysis test was done to learn more about the damage that this kind of accidents can originate in the human brain. Basically, some results obtained from real experiments were compared with the simulations performed with the updated head model.

Finally, several injury criterias were used for comparing the obtained data. These criteria take the physical parameters, like the accelerations and moments, and "translate" them into a value that allows to evaluate from a quantitative point of view the probability of suffering a fatal injury. In the present work, the following criteria were used:

- HIC: Head Injury Criteria
- MOC: Total Moment Occipital Condyle

1.3 Injury criteria

Injury criteria try to assess the real damage that certain accelerations and moments would cause to a human being. For the present project, these coefficients link the observed behaviour of the dummies in the simulations and the experiments to the real damage that the virtual experiment would have caused in the reality. To evaluate the damage in the human being, these expressions usually give a certain number as a result of the computation. This number makes possible to translate the numerical value of the criteria to a qualitative analysis of the damage caused, being possible to calculate the probability of suffering a fatal injury.

The mathematical expressions of the different criteria and their corresponding margins have been obtained by collecting plenty of data of different experiments with human corpses and observing the damage caused to their dorsal spine and brain after suffering a determined value of accelerations and mo-

ments. The expressions were deduced by means of statistical tools that tried to find out which parameters were involved in the appearance of those injuries(2). For the margins of the criterias, the procedure was to generate certain accelerations and moments in the corpses and evaluate if the injury caused was lethal from a biological point of view. After that, the corresponding value of the criteria was obtained in order to relate the qualitative valoration to the numerical one. Now a brief description of the criteria used during the thesis will be done.

1.3.1 HIC

It is the most common criteria for evaluating the head damage in short-time lapse impacts. This criteria is based on the time history of the accelerations that the centre of gravity of the head experiments along an interval of time. Originally, the criteria was developed from the Wayne State Tolerance Curve. This experimental tendency, obtained from the data collected in experiments with corpses, showed that there is a correlation between the admissible acceleration that the head can stand and the time pulse. Basically, if the time of application is increased, the mean acceleration that the head suffers is lower(3). Anyway, Wayne criteria was criticized because the number of data points used for elaborating the curve was limited and it was difficult to obtain exactly the same result for a parameter twice because corpses were not exactly equal. For this reason, researchers worked in another criteria that allowed them to increase the realiability of the results.

Then, the Head injury Criteria (HIC) was invented. The main difference from the previous one is that it works with the resultant of the acceleration, not only its frontal component. The expression of the criteria is the following

one:

$$HIC_{15} = max\left[(t_2 - t_1)\left(\frac{1}{t_2 - t_1}\int_{t1}^{t2} a(t)dt\right)^{2.5}\right] \tag{1.1}$$

$$a(t) = \sqrt{a_x(t)^2 + a_y(t)^2 + a_z(t)^2} \tag{1.2}$$

where $a(t)$ is the resultant of the acceleration along the time history and t_2 and t_1 are the different instants of time that will determine the limits of integration. These two instants do not have to coincide with the beginning and ending instant of the simulation, in fact, they never do it. They are usually two random times chosen during the pulse, it has been decided to use a HIC_{15} for this work so the difference between those two instants will be limited to $0.015s$ at most.

As it can be seen, the formula of the criteria contains a maximum function. This is because the time interval can be chosen randomly during the time pulse but with the condition that the proper time instants would be the ones that maximize the value of the criteria.

In the case of the HIC_{15} the maximum allowable value is 700, from this point the risk of severe injury is greater than 5% (1). The accelerations were processed by means of a CFC 1000 filter according to the regulation SAE J211(7).

1.3.2 MOC

MOC is the acronym of the *Total Moment about the Occipital Condyle*. It consists in calculating the value of the moment at the Occipital Condyle in relation with the moment calculated at a particular point. The moments around x and y are given by the expressions:

$$MOC_x = M_y - DF_x \tag{1.3}$$

$$MOC_y = M_x - DF_y \tag{1.4}$$

Where the M_i are the moments taken in the direction i, F_i are the forces in their respective directions and D is the distance between the load cell unit and the Occipital Condyle. In the Hybrid III dummy model, as there is no room to put the measuring instrument directly in the Occipital Condyle, it must be placed at the load cell unit for performing later a correction with the distance from the cell to the Occipital Condyle. According to the bibliography (5), the distance for the 50% male dummy with a Denton Load Cell model IF-205 is 0.01778 m. Anyway, it is not necessary to apply this criteria to the latest dummy model because the postprocessing documentation(6) indicates how to obtain directly the moments at the Occipital Condyle.

Following the regulation SAE J211 (7), a CFC 600 filter has been applied to the moments and forces for both models. Finally, the limiting values for this criteria are (1):

MOC	Maximum allowable value[Nm]
MOC_x	134
$MOC_{y_{extension}}$	57
$MOC_{y_{flexion}}$	190

Table 1.1: Allowable values of MOC

Chapter 2

State of art

In this chapter, a brief summary of the history of crash tests and dummies will be reviewed. Moreover, the specifications of the HIII dummy will be discussed. Finally, the two models of the head (LSTC.H3.103008_V1.0 and LSTC.NCAC_H3_50TH.130528_BETA) will be compared to see their main characteristics.

2.1 History of dummy crash

At the beginning of the last century, the amount of cars increased exponentially due to the fact that they became cheaper as new methods of production were introduced (assembly lines,improvements in the fuel...). The problem was that this industrial race didn't take care about the safety of the new automobiles that they were launching to the market so the number of deaths that had a relation with car accidents experienced a huge increase, achieving the rate of 15.6 deaths per 100 miles/vehicle in 1930.

Companies and research institutions realized that the safety of the passen-

gers should be a major priority. For this reason, Wayne University of Detroit started to look into these topics during the 30s. Initially, they performed experiments with human corpses in order to see the qualitative effects that a high velocity impact can have in the body of a human being. Furthermore they also implemented accelerometers in their bodies to do a more rigorous analysis of the injuries caused. Anyway, this procedure was finally refused because it was impossible to obtain bodies with the same weight and shape so the repeatability of the results could not be ensured. Furthermore, most of the corpses belonged to a really narrow segment of the population(old caucasic male) so it was necessary to obtain data for the rest of the groups in the society.

Some alternatives were also considered at that time. Due to the moral conflict that using human bodies in the experiments may cause, some researchers involved in these kind of investigations offered themselves to be part of the experiences. This was the case of Lawrence of Patrick, who studied the effects of the deceleration in the human being, and the Colonel John Paul Stapp, who also suffered the deceleration effects piloting a vehicle which could reach 1000 km/h. Another considered option was using animals in the experiments because it was easier to obtain the death body of a non-human being, the idea was quickly abandoned due to the fact that it was not possible to obtain a direct numerical comparison between the results of animals and humans.

Finally, the already mentioned Colonel John Paul Stapp, who was investigating the effect of an ejectable seat that he made, wanted to have a device similar to the human body to know the effects of the seat over the human body. The company Sierra engineering answered with a dummy model (Sierra Sam) in 1949, which was used for the experiments in the automotive and aircraft industry. This model was a 95% dummy, so only 5% of the males at that time had a larger weight and height that the one of the model. This shows that the first dummies were not really sophisticated and the data that they provided could not be extrapolated to most of the people characteristics. Some years later, the engineer Samuel Andelson created the V.I.P model, which was

specially made for the tests of General Motors and Ford.

Anyway, none of these dummies could convince the engineers of GM, who decided to develop a new reliable and durable dummy, the Hybrid I was created in 1971. This dummy was a 50% male model, which means that it represents the average adult men. This dummy was the result of the mixture between the V.I.P and the Sierra Stan, which was a new model that Sierra engineering had produced in the previous years. The Hybrid I dummy quickly resulted to be obsolete, this encouraged the engineers to develop the Hybrid II. This new model already included the different body joints and the vertebral spine, moreover it was the first one to accomplish the standards (American Federal Motor Vehicle Safety Standard -FMVSS) for experiments with safety belts.

Figure 2.1: Image of the Hybrid II

After that, the model that revolutionated the industry arrived in 1976, the Hybrid III. This dummy supposed an inflection point in the crash test history, being still used nowadays. Its details will be discussed in the following section.

2.2 Hybrid III

The Hybrid III 50th Percentile Male is the most widely dummy device used along the world in crash testing. Originally developed by General Motors, the Hybrid III 50th is now mantained and developed by Humanetics with the Society of Automotive Engineers'(SAE) Biomechanics Commitees and the National Highway Transport and Safety Administration (NHTSA). The dummy is a regulated test device in the USA Code of Federal Regulations and also in the European ECE Regulations. It is considered to have excellent biofidelity and instrumentation capability.

The main differences that this model introduces are the segmented neck made of rubber with an internal cable going through it. This modification provides a better recreation of the moment rotation response. Furthermore, human chest deflection can be simulated by means of six high strength steel ribs, the interaction with shoulder belts is also improved by the changes introduced in the clavicae and scaple. The recreation of the human position when it is seated is achieved by means of the implementation of a curved cylindrical rubber lumbar spine.

Figure 2.2: Image of the family HIII

It is also important to remark that these dummies have a wide range of instrumentation embebbed, achieving the astonishing amount of 44 devices distributed along the body. In the case of the present work, the instrumentation used were the accelerometers (a_x,a_y,a_z) of the head and a 6-axis Upper Neck Load Cell. Furthermore, one of the advantages that this new model of dummy offered was the implementation of models for kids, so data of the biomechanical behaviour related to the children could be gathered now, being the dummies elaborated by extrapolation of the expected behaviours. The characteristics of the family are:

Model	height(cm)	weight(kg)	sitting height(cm)
95% male dummy	188	101.1	93.5
50% male dummy	175	77.2	88.4
5% female dummy	152	49.2	78.7
10 years old kid	-	32.4	71.9
6 years old kid	-	23.4	63.5
3 years old kid	-	15.5	54.6

Table 2.1: Family HIII data given gy the IIHS and (8)

2.3 Finite element models

In the current work, it has also been used the digital version of the HIII dummy for FE softwares. The advantage that these kind of simulations offer is that the experiments could be performed in a much faster way and the money spent for doing them will be much lower than the one that would be spent doing them in the reality. Furthermore, the simulations ensure a larger knowledge of all the factors involving the experiment and the capability to reproduce the experiments in identical conditions. Anyway, real experiments with the dummies can not be avoided because these models are not reliable yet, so

real data are needed for having a correct setting of the parameters involved in the analysis. The old model is the 50th HIII male dummy's head, created by the Livermore Software Technology Corporation(LSTC) and modified at LaST. The external viscoelastic part of the head plays the role of the skin while the inferior rigid parts are the skull, moreover we have the upper load cell in the lowest part of the skull. After that, there is the revolute joint between the head and the neck which regulates the relative movement between them and the possible forces that may appear. Finally, the neck is formed by several solid rigid parts recreating the cervical disks while the connection between them is regulated by a viscoelatic part. For giving the neck some stiffness, and helping to recreate the real behaviour, a beam part goes through the neck. On the other side, the LSTC.NCAC_H3_50TH.130528_BETA dummy's head is much more complex.

This model is formed by a divided skull that recreates the real head of the HIII dummy, as it also has a divided head in order to remove its rear part for introducing the measuring devices. In this case, we have two layers of viscoelastic skin on the front and the rear part of the head, consequently there will also be two parts of the skull. One difference between this model and the previous one is that it tries to simulate all the deformations that may happen inside the head so the parts that were rigid, like the skull, are elastic in this one. Obviously, this will increase the computational cost but the results obtained will be more accurate. The joint between the head and the neck is also improved in this model, perfomed by joining two parts belonging each one of them. Regarding the neck, the structure is similar to the previous model, having intercervical disks and a rubber that connects them. Furthermore, it also has an internal cable that tries to recreate the stiffness of the neck. Here we can see an image of both heads:

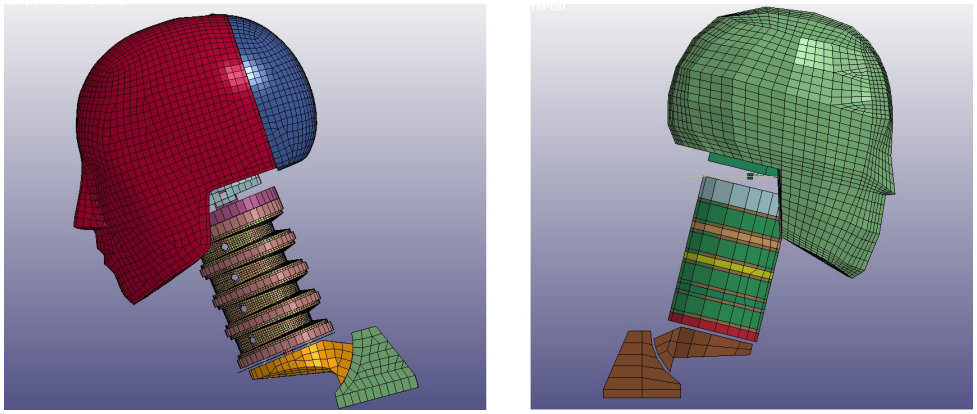

Figure 2.3: Image of the old model of HIII(right) and the 2016 model (left)

Finally, it is important to remark the different ways to reproduce the instrument implementation in the dummy for each model. In the LSTC.H3.103008_V1.0 model, the instrumentation is represented by a solid block placed inside the skull, which plays the role of the accelerometer, and the upper load cell, where no instrument can be placed in the reality so moments and forces are measured from a higher point as it has been explained in the last section. In the LSTC.NCAC_H3_50TH.130528_BETA model, the recreation of the instrument positioning has been improved, being actually really similar to the one inside the HIII dummy's real head. For this model, the cube representing the accelerometer is placed inside the head on its corresponding mounting, two ballasts are placed on each side of the head to avoid that any part of the head hits the instrument. A descriptive image has been added to make it clear:

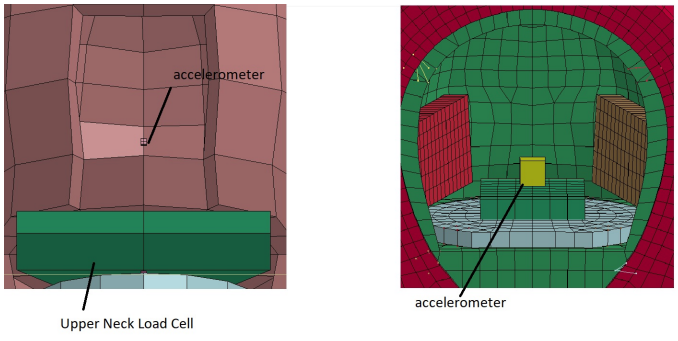

Figure 2.4: Image of instruments in the new head (right) and in the old (left)

Chapter 3

Experimental results

In this part of the project the experiments that were performed for obtaining real results of the dummy's behaviour will be detailed. This data will be compared with the results obtained in the simulations to see if the setting of the virual parameters is close to the real one. In the first part, a brief summary of the experiment performed at the paper (1) of the bibliography will be done and its main results will be exposed. In the second part, the head drop test performed for the present thesis will be explained, introducing its main results. Both experiments were conducted at LaST lab (Politecnico di Milano)

3.1 Pendulum striking against head

This experiment was done in order to see the way that the Hybrid III dummy reacts when it suffers an external hit to its head at a given velocity for different incident angles of the skull. All this collected data could be also used for improving the reliability of the simulations using LS-DYNA. In this experiment, the head of the 50th Hybrid III male dummy was used. The instrumentation implemented allowed to measure the three linear accelerations of the head's

centre of gravity, angular displacements and the six upper forces and moments. To measure this, three accelerometers were installed inside the skull of the ATD for measuring the linear acceleration, the three forces and moments were measured by a 6-axis Upper Load Cell. The angular velocity was obtained by a three axis DTS ARS-rate gyroscope installed on the head's centre of gravity.

The head was hitted by a cylindrical impactor that was characterized by a mass of 23.1 kg, a radius of 0.075 m, a length of 0.7 m and a height of ground of 0.737 m. The impactor was pinned by eight cables in a way that the pendulum moved only in the horizontal direction. All the collected data was processed by an adquisition software for applying the corresponding filter later, following the rules given at the document SAE J211. It is also remarkable to say that the neck had a cable going through it, so the experiment tried to see also the influence of this cable over the head's behaviour. Changes on the tension of this element induced a variation on the plane D angle (plane situated at the base of the skull). For the first state of tension, the head was completely horizontal while for the second one a variation of 7 degrees could be observed, an image of the recalled experiment has been attached in order to clarify the concept (1):

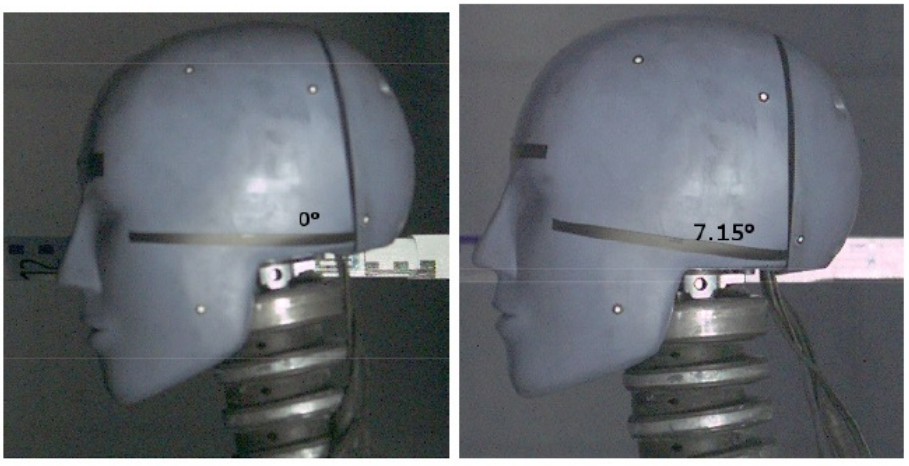

Figure 3.1: Image of the two different Plane D angles used in the experiment

Regarding the test procedure, the pendulum was initially released to hit

the head at a constant velocity (1.428 m/s) in the three different orientations (front, lateral and upper) and in both cable configurations. In order to ensure the repeatability of the results, the experiment was performed three times for each combination of orientation and cable configuration, releasing always the pendulum from the same position. Data was collected and postprocessed with MATLAB, applying the corresponding CFC filters to each parameter according to the regulation SAR J211. After that, the main results were plotted and compared in MATLAB, looking for a low dispersion of the results that belong to the same combination of configurations. For the present work, the interesting data was the one obtained from the frontal impact experiments because it was the only one that could be used to compare with the simulations. The first number of the tests in the legend of the results indicates the position of the head in the experiment (horizontal or with 7 degrees, respectively) and the second one proves the number of attempt with that configuration:

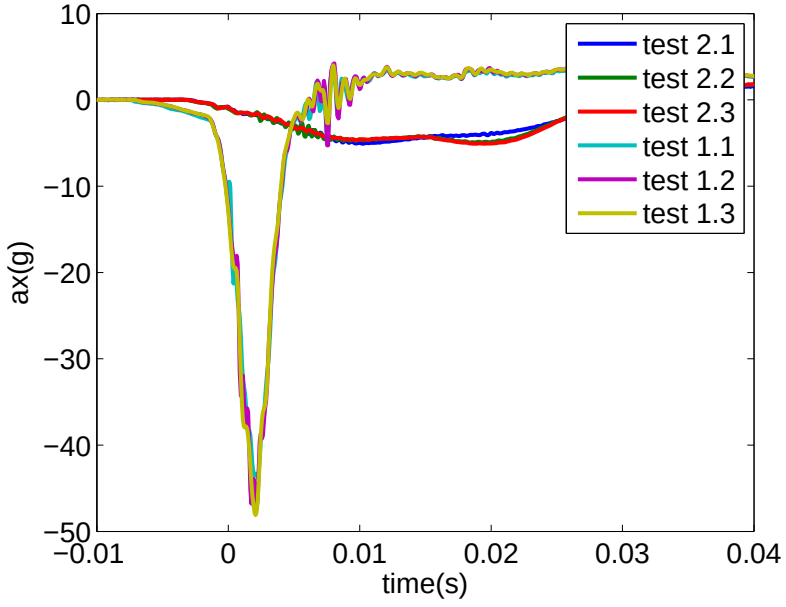

Figure 3.2: Image of the results of the frontal accelerations

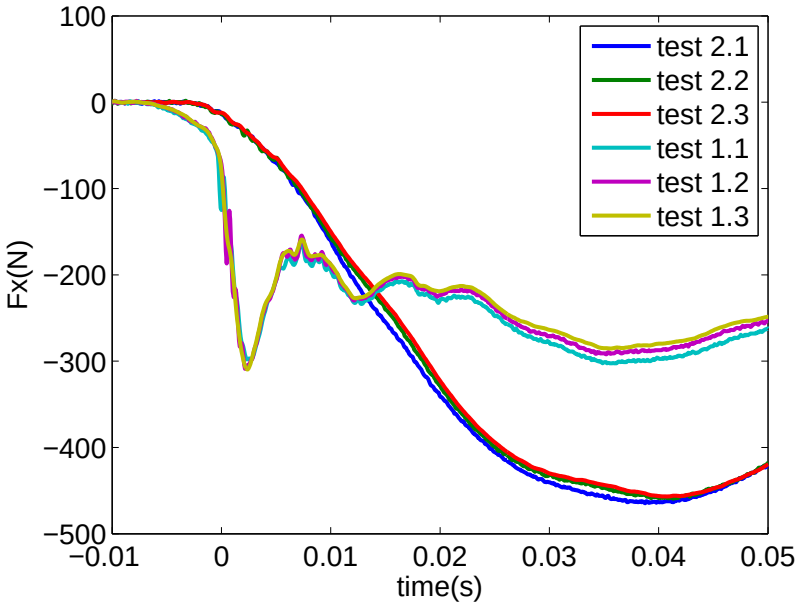

Figure 3.3: Image of the results of the frontal forces

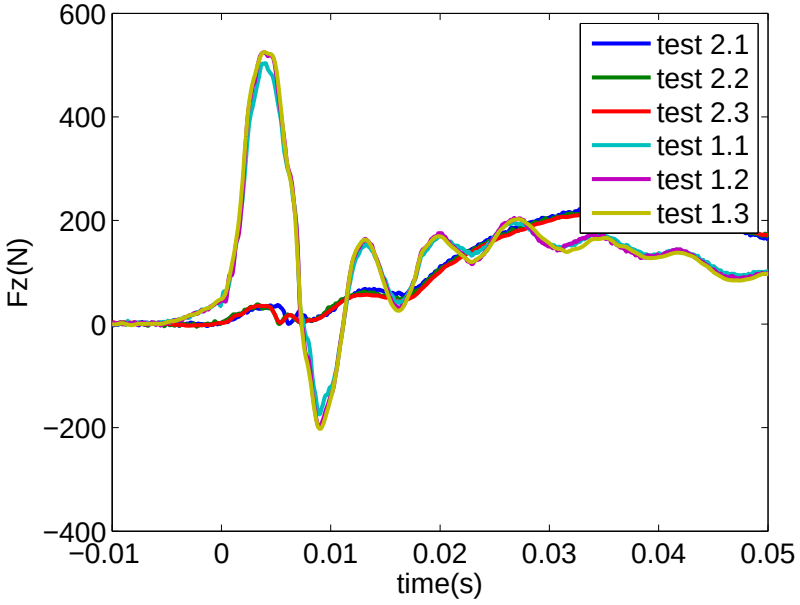

Figure 3.4: Image of the results of the vertical forces

As it has been proved, for the frontal impacts the most important parameters are the acceleration and the force on the x axis. The results seem to be qualitatively well because the head suffers an initial negative acceleration, induced by the inertial movement of the pendulum that becomes quickly

damped by the effect of the neck recovering its initial position. It can also be observed the strong influence of the head's position, which has been modified by the action of the neck cable. For the first case, the one with 0 degrees of inclination, it can be seen that the inertial force is transmitted better to the head than in the second one, as it reaches a higher peak of acceleration. An error between its maximum values for both configurations was calculated to know the possible dispersion that may exist:

Test	max(ax(g))	error
Test 1.1	43.7638	-
Test 1.2	47.3928	8.29%
Test 1.3	48.1108	9.99%
Test 2.1	10.4938	-
Test 2.2	9.7122	8.047%
Test 2.3	9.4269	10.166%

Table 3.1: Maximum values of the a_x and the error respect the first test of each configuration

The error observed stands along 10 % so the repeatability of the experiment can be ensured as the number is still low. Finally, the analysis of the injury criteria was implemented in order to see if the accelerations and forces used in the experience did not cause any fatal damage to the dummy. First, the HIC was calculated for the different tests, being the frontal acceleration the most important component and the lateral one nearly negligible. The graphics of the MOC and Nij were also calculated and plotted, these graphics can be found at the Appendix B of the bibliography (1). It can be advanced that none of this parameters are close to overpass the limits stated on the first chapter of the present thesis due to the low velocity of the pendulum. The values obtained for the HIC will be attached now:

The error calculated in the previous table has been found because a new

Test	HIC	error
Test 1.1	19.877	0.019%
Test 1.2	21.8095	0.26%
Test 1.3	22.2501	0.44%
Test 2.1	1.4030	0.071%
Test 2.2	1.1911	0%
Test 2.3	1.1269	0%

Table 3.2: HIC values and error with respect bibliography(1)

algorythm for the calculation of the coefficient has been programmed in MATLAB so it was necessary to validate the code with some reliable data, like the one provided in the bibliography. The difference between the results in (1) and the ones found out is negligible so the code can be considered valid. As a remarkable fact, it can be said that the HIC decreases a lot from the first cable configuration to the second one.

3.2 Head drop tests

These experiments were done at the LaST lab for the present work. As before, they were performed to have a set of experimental data to compare with the simulations carried out in the present work. In the experiments, different heights were tested, including several relative inclinations of the head respect the horizontal plane. Anyway, the experiment was performed with the head separated from the rest of the body so the results obtained can not have a direct relation with the real human body response because it is a situation that can not be found in the reality. Despite of this, the experiment is important in order to perform a correct tuning of the parameters of the simulation, having a realistic model that allows to obtain accurate results for those experiments

with a higher importance from the biomechanical point of view.

3.2.1 Assembly of the experiment

It was prepared based on the calibration test detailed in the bibliography (10). First, the head with the neck transducer structural replacement was separated from the rest of the 50th male Hybrid III dummy. After that, three accelerometers in each main direction were positioned inside of the head. According to their position, the X axis pointed towards the nose, the Y axis was oriented in a lateral of the head and the Z axis pointed where the cervical spine would be. The head was suspended on a crane that allowed to change easily the height of the head by a system of belts and ropes.

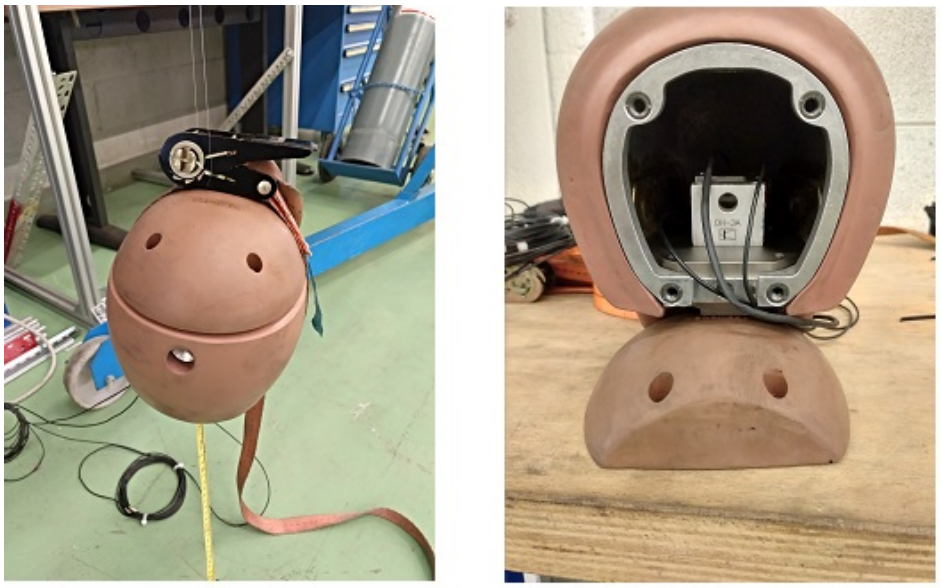

Figure 3.5: Images of the experiment assembly

As it can be seen, the belt occupied a relative important volume respect the head so its mass was measured in order to know if it could influentiate the acceleration results:

assembly	weight(kg)
head	4.333
head and belt	4.548

Table 3.3: Weights of the head and the belts

The weight of the belt is around 0.215 kg. It can be calculated that it represents approximately the 5% of the head's weight so the belts will have some influence on the results but it was considered to be the best system to orientate the head in the space, the variations on the acceleration results will be neglected in consequence.

3.2.2 Instrumentation

For the present experiment, three different accelerometers with a measurable range of 250 g were mounted inside the head at each main direction. Their specific reference numbers are: V1409J, W120GH, W120GD.

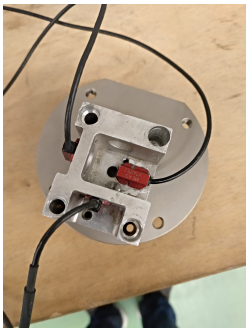

Figure 3.6: Image of the instrumentation used

3.2.3 Test procedure

The head was suspended from the crane by means of a rope tied to the belt. Once it was proved that the rope was able to resist the head's weight, we started manipulating the rope and the belt together in order to achieve the distance between the front of the head and the nose as specified in the standard (4), which is 12.7 mm. It is important to remark that, even if regulation specified that the front must had a lower position respect to the nose, it was also proved the inverse option in order to have a better understanding on the phenomena.

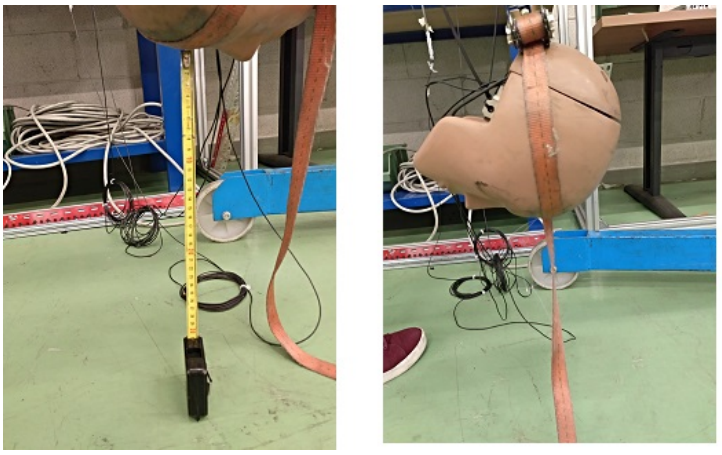

Figure 3.7: Images of the two relative position adopted. The one on the right is the specified on (4)

After positioning correctly the head, its height respect the floor could be modified manipulating the crane that held is. The regulation established that the distance between the front of the head and the floor should be 37.6 mm, but another height was also proved (200 mm) for observing how this variation affects on the studied parameters. Each combination of height and inclination was proved three times for ensuring the repeatability of the experiments. The results were recorded using a TDAS pro data adquisition system with a sampling frequency of 12500 Hz, where the accelerations a_x, a_y, a_z were captured from the channels 1,3,6 of this device. Then, the data obtained in the experiments were analysed in MATLAB in order to see the peaks of the accelerations in the three axis and its resultant after applying the CFC filter

(600, own citeria).

3.2.4 Results of the experiments

The results that are going to be presented have been obtained after removing the corresponding offset of the accelerations, measured due to the residual voltage captured by the adquisition device:

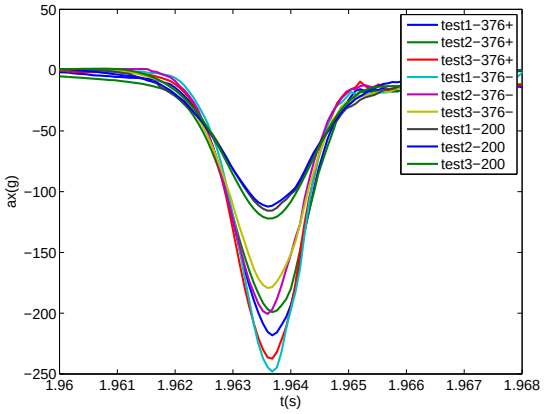

(a) Acceleration in x

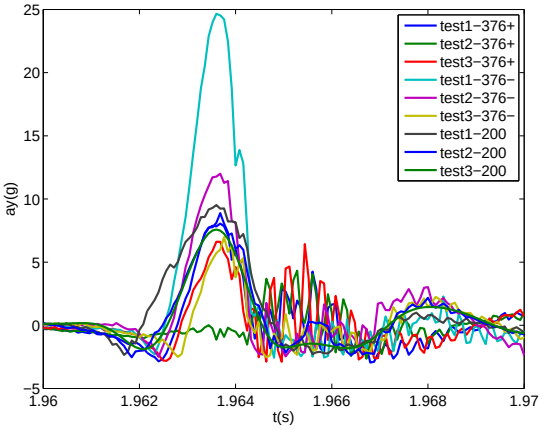

(b) Acceleration in y

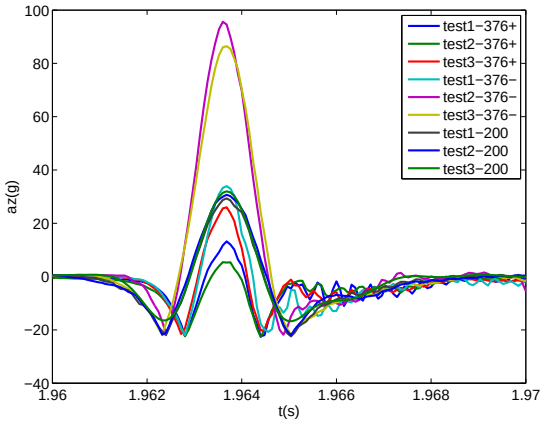

(c) Acceleration in z

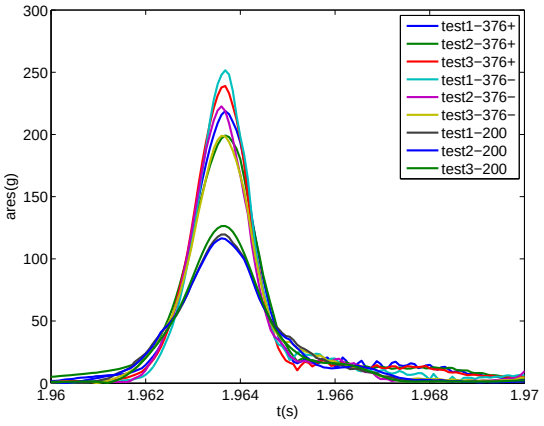

(d) Resultant acceleration

Additionaly, the figures of the acceleration peaks have also been found in order to have quantitative magnitudes to compare the results:

Test	$a_x(g)$	$a_y(g)$	$a_z(g)$	$a_{res}(g)$
Test1-376+	-218.224	8.880	5.341	218.804
Test2-376+	-199.138	20.346	13.22	199.207
Test3-376+	-237.477	9.533	25.987	238.986
Test1-376-	-248.111	24.655	33.931	251.6201
Test2-376-	-200.666	12.002	95.604	222.588
Test3-376-	-179.272	6.976	86.484	198.933
Test1-200	-115.684	9.514	29.341	119.578
Test2-200	-112.277	15.593	30.692	116.470
Test3-200	-122.084	7.582	31.992	126.377

Table 3.4: Acceleration peaks for the different tests

In the previous graphs, the notation $376+$ is related with the experiments where the nose was lower respect the front of the head, those ones labeled with $376-$ were the ones which nose relative position respect the front were negative. The rest of the experiments were performed at 200 mm. The figure that goes with the word "test" indicates the number of experiment with that specific configuration. As it can be seen, there is a huge difference between the peaks of the accelerations for the cases of 376 mm and 200 mm. First, it can be observed that when the height increases the maximum acceleration value also does it. Furthermore the dispersion of the data that it has been obtained is quite important, being the lateral acceleration an example of this. For that magnitude, there are some results that are three times larger than other ones (comparing between experiments with the same configuration). For this reason, it can be deduced that the amount of the experiments performed for each combination of height and inclination is not enough, being necessary to perform at least 2 additional experiments for each one. Anyway, results have been considered valid because the resultant acceleration offer an error that can be considered to be within the acceptable range (around 25%). This

range may seem to be high but it has been decided to use the data applying a personal criteria. Finally, it can be remarked that the most reliable set of experiments are the ones peformed for 200 mm because they show a lower difference between its maximum peaks(around 8.5%).

Regarding the qualitative results offered in the plots, it can also be seen that the inclination of the head offers a remarkable difference in the results. The main variation that may exist could be that for the acceleration in the Z axis, those with the nose lower respect to the front have lower results than the other case (approximately the half). Furthermore, the lateral acceleration is decreased also. Anyway, these details will be appreciated better in the plots of the mean curve for each set of tests:

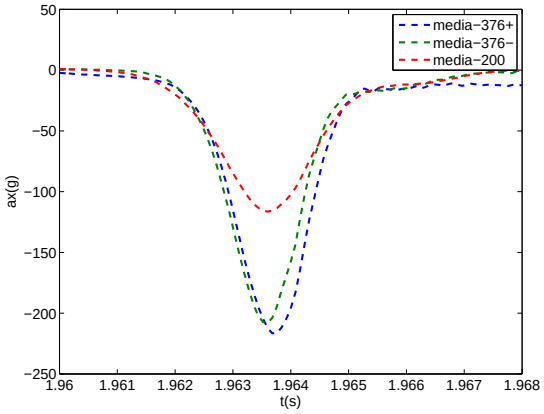

(e) Mean acceleration in x

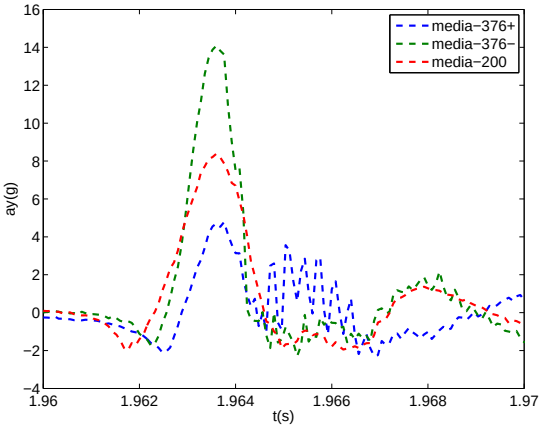

(f) Mean acceleration in y

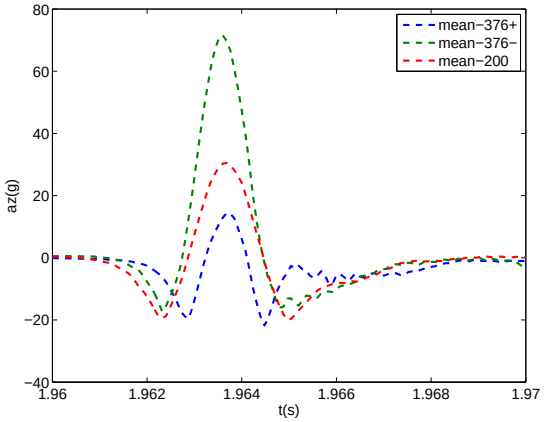

(g) Mean acceleration in z

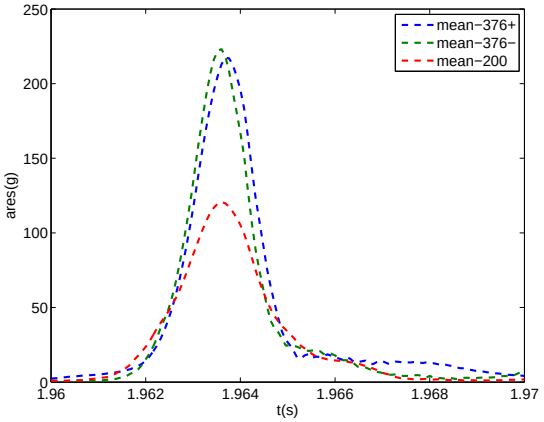

(h) Mean resultant acceleration

It can also be remarked that for the calibration case, the one at 376 mm and negative inclination, the specifications in the standard state that the peak of the acceleration must be between 225 g and 275 g while the lateral acceleration must be under 15 g. For the results of the experiments. it has been obtained that the mean lateral acceleration peak is 14.08 g while the resultant is 223.1 g. The first figure is within the range stablished by the bibliography while the second one diverges in a 0.84% from the accepted value. Due to the small errors it can be considered that the results accomplish the specifications stated. Finally, the HIC injury criteria has also been calculated for each case:

Test	HIC
Test1-376+	595.486
Test2-376+	506.164
Test3-376+	684.343
Test1-376-	718.174
Test2-376-	559.770
Test3-376-	467.208
Test1-200	158.948
Test1-200	153.529
Test1-200	180.595

Table 3.5: Acceleration peaks for the different tests

As it can be seen, the divergence of the criteria's value for the tests with the same initial characteristics increase for those ones performed at higher heights.

Chapter 4

Simulations and results

In this chapter, the simulations performed for the present project will be discussed and their results commented. In the first part, the curves obtained in the simulations performed for the case of the head being striked by a pendulum will be studied deeply, observing the main results for the sensitivity analysis performed. Then, an equivalent study will be done for the case of the head drop .

4.1 Pendulum strike

In these simulations, the complete head with the neck of the 50th male LSTC.NCAC_H3_50TH.130528_BETA model was placed in front of a pendulum that recreated the one used in the experiments. It was composed by a main cylindrical body pinned by eight cables that were positioned on a certain way according to the required impact speed of the pendulum, this model was taken from the thesis (1) of the bibliography. The head was placed as close as possible to the pendulum's body in order to reduce the time spent for the simulation. The pendulum's velocity was the same used in the experiments:

1.428 m/s.

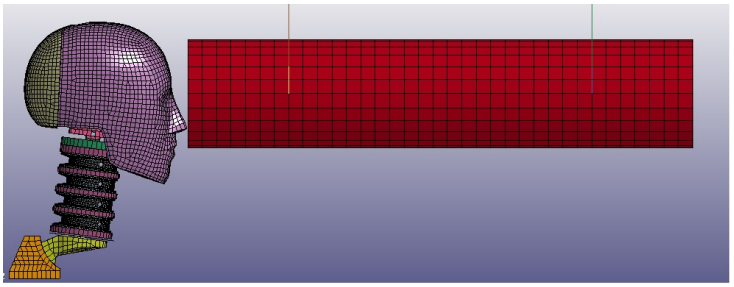

Figure 4.1: Simulation assembly for the pendulum strike

The results obtained were always compared to the experimental ones, applying the corresponding CFC filters (1000 for the accelerations and angular velocities and 600 to the other magnitudes). It was appropiate to know the default values of the parameters involved in each material of interest due to the :

Material	ρ $(\frac{kg}{m^3})$	E(MPa)	G_0 (MPa)	$G_I(MPa)$	B(MPa)	decay
1000000	$1.2 \cdot 10^3$	-	30	0.6	25.6	250
1000002	$2.7 \cdot 10^3$	$7.0 \cdot 10^4$	-	-	-	-
1000006	$7.89 \cdot 10^3$	$2.0 \cdot 10^5$	-	-	-	-
1000009	$7.89 \cdot 10^3$	$2.0 \cdot 10^5$	-	-	-	-
1000010	$1.0 \cdot 10^2$	50000	-	-	-	-
1000011	$1.1 \cdot 10^3$	-	4.6	1	112.8	110
1000012	$2.71 \cdot 10^3$	$7.0 \cdot 10^4$	-	-	-	-
1000015	$2.71 \cdot 10^3$	$7.0 \cdot 10^4$	-	-	-	-
1000017	$1.40 \cdot 10^3$	5800	-	-	-	-
1000018	$7.89 \cdot 10^3$	800	-	-	-	-
1000019	$7.89 * 10^3$	$2.0 * 10^5$	-	-	-	-
1000020	$7.89 * 10^3$	$2.0 * 10^5$	-	-	-	-
1000021	$7.89 * 10^3$	$2.0 * 10^5$	-	-	-	-

Table 4.1: Default values of the materials

Among all the magnitudes obtained, it has been decided to include in the report only the frontal acceleration (a_x), the frontal and vertical forces (F_x and F_z) and the Total Moment at the Occipital Condyle in $Y(MOC_y)$ because they are the most important from a physical point of view. The results obtained for the default parameters of the materials are depicted in the following graphs:

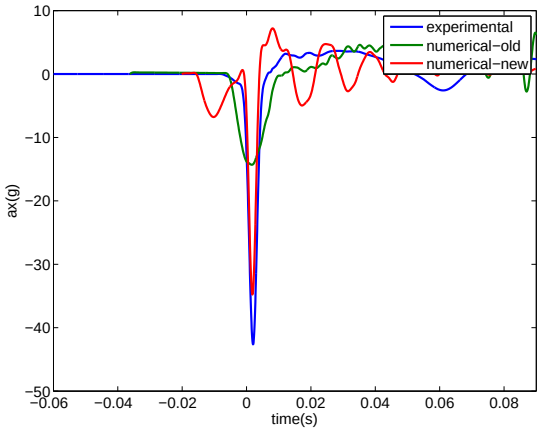

(a) Accelerations in x(g)

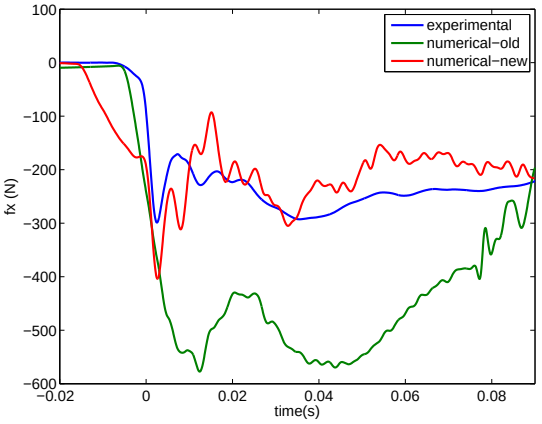

(b) Force in x(N)

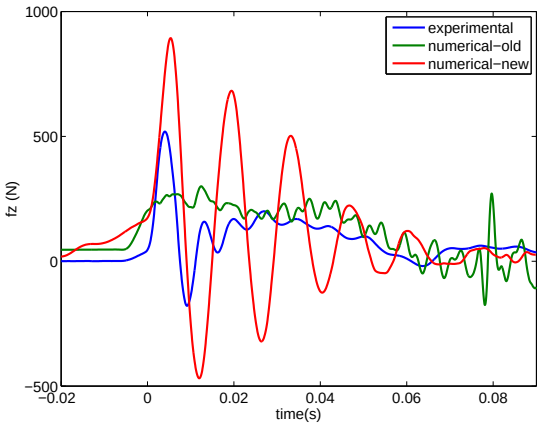

(c) Force in z(N)

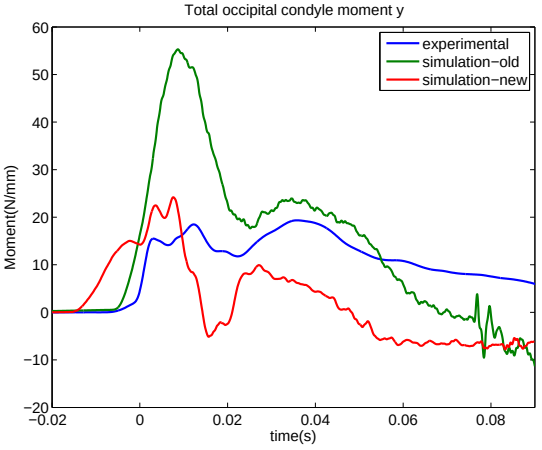

(d) Total moment in y(N)

The obtained figures are really interesting. First, it should be mentioned that the noise observed in the graphs was really high so an additional CFC180 filter was applied to reduce it. In general, it can be observed that the behaviour of the new head (LSTC.NCAC_H3_50TH.130528_BETA) recreates better the experimental response than the old one (LSTC.H3.103008_V1.0). For the

acceleration graph, it can be observed that the maximum peak of the new model is closer to the experimental one. Furthermore, it can also be seen that in the curve of the new model there is a small peak before the main one, this is because the simulation was able to capture the acceleration produced by the deformation of the nose after the first impact. The main peak was originated after the impact of the pendulum with the front. Regarding the frontal force, it can be observed that there is a main discontinuity produced by the initial impact of the pendulum that moves the head backwards. The force on the vertical axis shows a rebound that damps after a certain amount of time, it can also be observed that these oscillations are higher for the new model head while the old one is not able to capture them. Finally, it can be observed that the correlation between the new model and the experiments is higher than the one obtained with the old head for the Total Moment over the Occipital Condyle. From a quantitative point of view, it has been decided to report the maximum values of each variable and the HIC in order to have a better idea of the differences that may exist:

Simulations	a_x(g)	f_x(N)	f_z(N)	$MOC_y(N \cdot m)$	HIC
old	-14.3051	-577.3471	300.0350	55.2923	22.4872
new	-34.7715	-404.0127	893.6105	24.1918	11.9938
experimental	-43.8016	-298.8356	519.5586	19.3578	20.5755

Table 4.2: Maximum values of the variables and HIC

Several "boundary" parameters were analysed before performing the sensitivity analysis. First, it was studied if the position of the system of reference with respect to the instrument placed at the c.g. influentiated significantly the results of the accelerations. The S.R. was placed in two different positions to observe the possible deviations originated: the skull and the cube representing the intrumentation. The results obtained were the following ones:

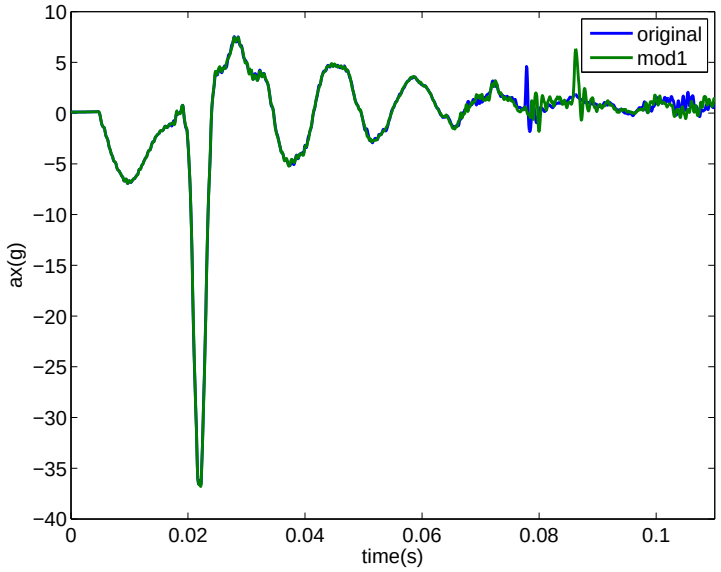

Figure 4.2: Acceleration results for the different S.R.

As it can be seen, the differences that may exist are negligible so the S.R. was placed on the instrumentation cube. After this, it was also increased the amount of elements in the pendulum in order to see if the results varied in some way. The final curves were:

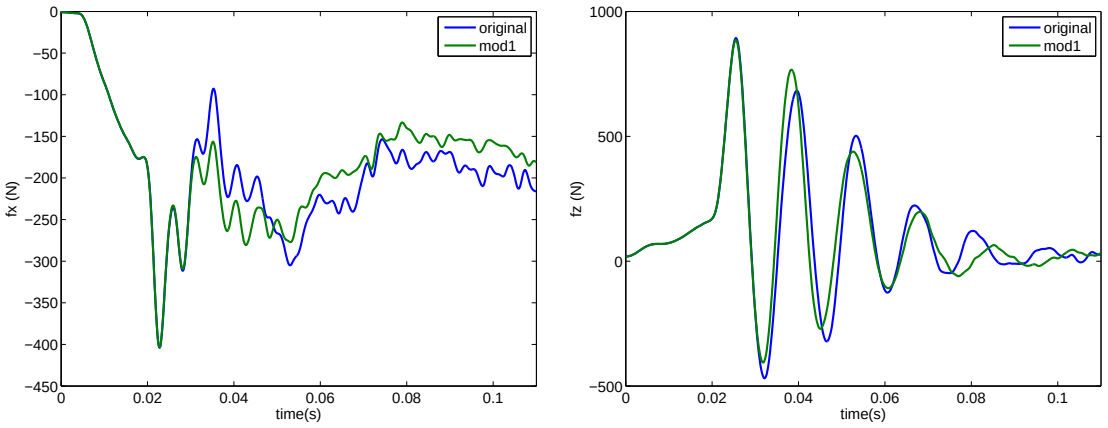

(a) Force in X(N)

(b) Force in z(N)

In this case, the results show that a slight difference may be originated. Anyway, those differences were not relevant for the final results so it was decided to use the option with a lower amount of elements at the pendulum because it permitted to reduce the computational cost of the simulation.

4.1.1 Sensitivity analysis

This study consisted in changing the values of the parameters that defined each material in order to know the possible influence that they may cause in the resultant variables of interest (accelerations, moments, forces...). The studied materials were the ones that defined the head skin (1000000 and 1000001), the skull (1000002 and 1000010), the head base (1000006), the joints of the head (1000009), the neck rubber (1000011), the upper part of the neck (1000012), neck disks (1000015), inferior part of the neck (1000017), the neck cable (1000018) and the neck joints (1000019,1000020,1000021). The rest of the materials were used for defining auxiliary parts or the instruments so they were not considered to be relevant for the results.

Head material- 1000000

It was the viscoelastic material used for the part of the head skin. In this case, it was considered to be interesting because it defined the material of the first part to impact with the pendulum. Its behaviour was characterized by the infinite shear modulus(G_I), the short-time shear modulus (G_0), the bulk modulus (B), the density (ρ) and the decay constant. The first variable checked was the bulk modulus, being the green curve the one of 50 MPa and 100 MPa the red one, obtaining the following results:

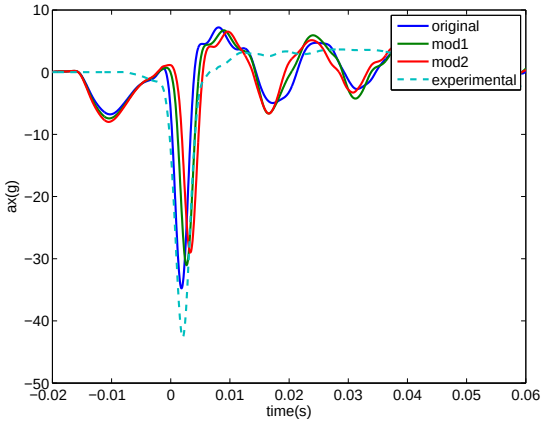

(c) Accelerations in x(g)

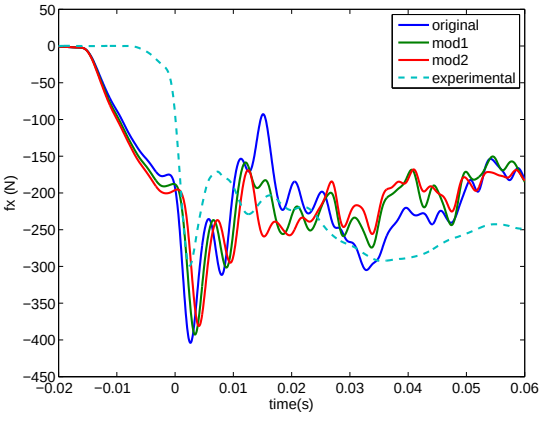

(d) Force in x(N)

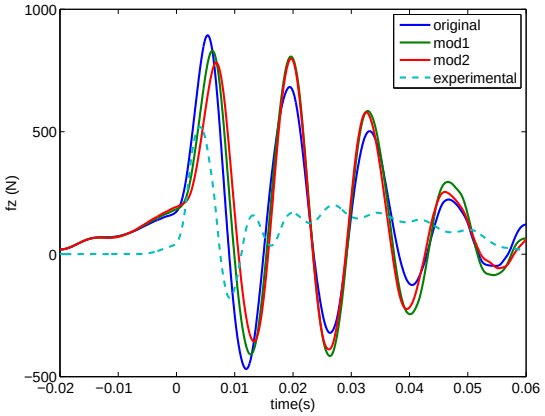

(e) Force in z(N)

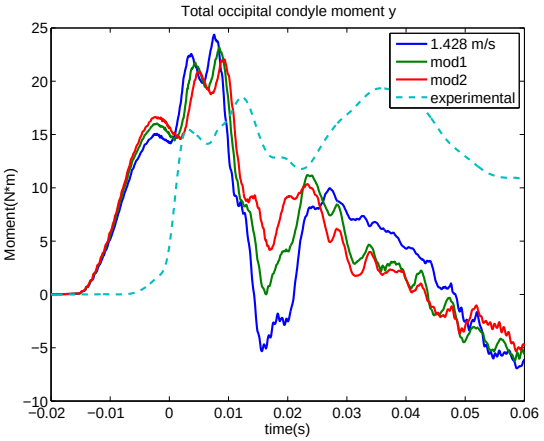

(f) Total Moment in y (N*m)

B(MPa)	a_x(g)	F_x(N)	F_z(N)	$M_y(N \cdot m)$
25.6	-34.7715	-404.0127	893.6105	24.3701
50	-31.0394	-392.7562	830.6105	23.1631
100	-29.009	-381.1389	798.8790	22.0519

Table 4.3: Maximum values of the variables

It can be observed that the bulk modulus affects sensitively the values of all the considered variables. The studied values of this parameter were in both cases higher than the default value because the bulk modulus could not be lower than $\frac{2}{3}$ of the G_0, being the original value already on the limit. Bulk modulus has a non-linear relation with the different resultant variables. For higher values of B, it is obtained that the peaks of the accelerations, forces and moments decrease.

After this, the possible influence of the density on the material was studied. For this reason, it was decided to perform small variations of the default value ($\pm$ 0.5·10^3 kg/m^3) in order to see if some realistic change of the original material could lead to an interesting result. The variances were small because larger changes would have led to completely different materials, changing drastically

the model. For example, it would have no sense to change the density of a rubber material for the one of an iron. Therefore, the curves obtained were the following ones, being the green one the corresponding to $0.7 \cdot 10^3 \ \frac{kg}{m^3}$ and the red one related to $1.7 \cdot 10^3 \ \frac{kg}{m^3}$:

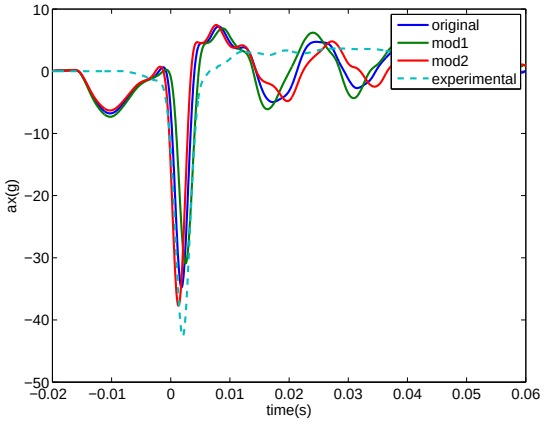

(g) Accelerations in x(g)

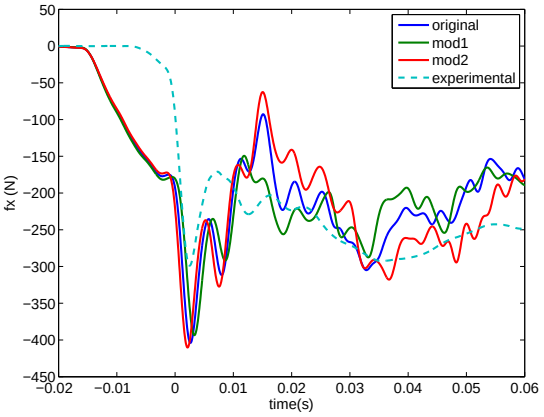

(h) Force in x(N)

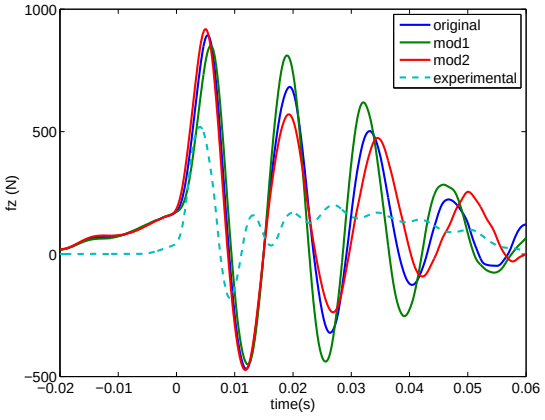

(i) Force in z(N)

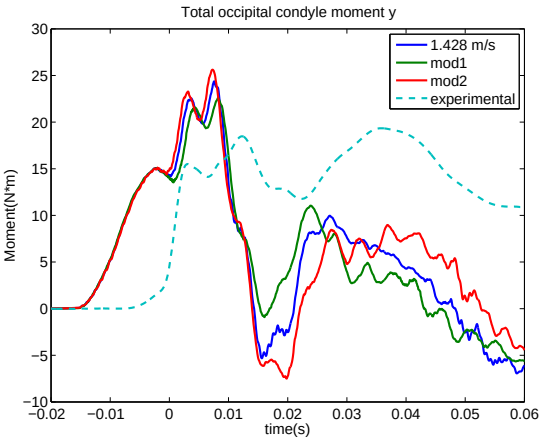

(j) Total Moment in y (N*m)

$\rho(\frac{kg}{m^3})$	a_x(g)	F_x(N)	F_z(N)	$M_y(N \cdot m)$
$0.7 \cdot 10^3$	-30.9153	-393.4946	850.4680	22.5983
$1.2 \cdot 10^3$	-34.7715	-404.0127	893.6105	24.3701
$1.7 \cdot 10^3$	-37.7161	-410.3715	918.2547	25.6227

Table 4.4: Maximum values of the variables

In this case it can be observed that the maximum values of the variables have more or less a linear variation with respect to the density. This is due to the fact that an increment of this parameter produces an increment in the mass of the model, changing the inertial properties consequently. Furthermore, if the density of the skin is increased, the force transmitted to the instrumentation cube by the pendulum is larger, so the acceleration registered will be bigger too.

The next studied parameter was the decay constant of the viscoelastic material. In this case, two different values of the parameter were proved, being the associated value of the green and red curve 2500 and 25 respectively:

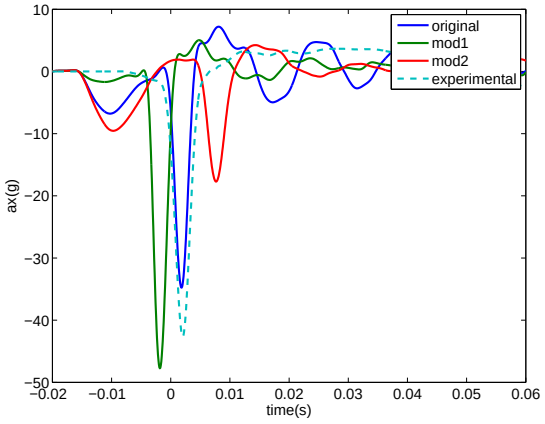

(k) Accelerations in x(g)

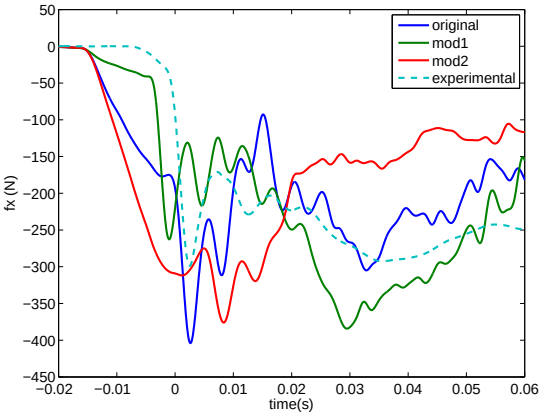

(l) Force in x(N)

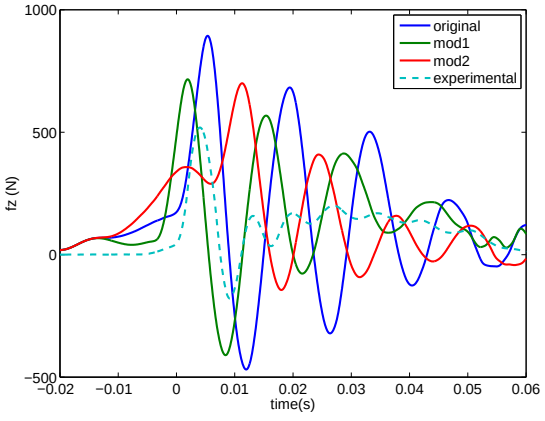

(m) Force in z(N)

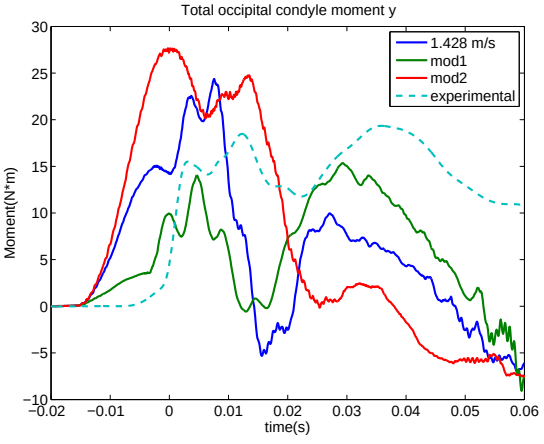

(n) Total Moment in y (N*m)

decay($1/s$)	a_x(g)	F_x(N)	F_z(N)	$M_y(N \cdot m)$
25	-17.7154	-375.9841	699.7892	27.6668
250	-34.7715	-404.0127	893.6105	24.3701
2500	-47.7480	-384.1980	715.9987	15.3489

Table 4.5: Maximum values of the variables

As it can be observed, the modification of the decay constant produces huge variations on the results obtained. Looking at the formulas that define the behaviour of the material in the theory manual(9), it can be found that the constitutive relations for this case are:

$$\sigma_{ij} = \int_0^t G(t-\tau)\frac{\partial \epsilon_{ij}}{\partial \tau} d\tau \tag{4.1}$$

$$G(t) = G_\infty + (G_0 - G_\infty)\exp^{-\beta t} \tag{4.2}$$

Where β is the decay constant, G_0 is the short-time shear modulus, G_∞ is the infinite shear constant and ϵ is the deformation that the σ generates. Increasing the decay causes an exponential reduction of the shear relaxation modulus due to the relation that can be seen in 4.2. This produces an increment of the measured deformations in the head because the external stress applied remains constant (force transmitted by the pendulum), causing a larger acceleration. Furthermore, the forces and the moments decrease if the decay constant is increased. Finally, it should be remarked that the results obtained for the decay constant 2500 fit quite well with the experimental results, diminishing also the first peak of the frontal acceleration originated by the nose deformation (which was not perceived in the experimental results).

Finally, the infinite shear modulus (G_∞) was analysed for observing the possible variations that it could produce. Two different values were also checked:

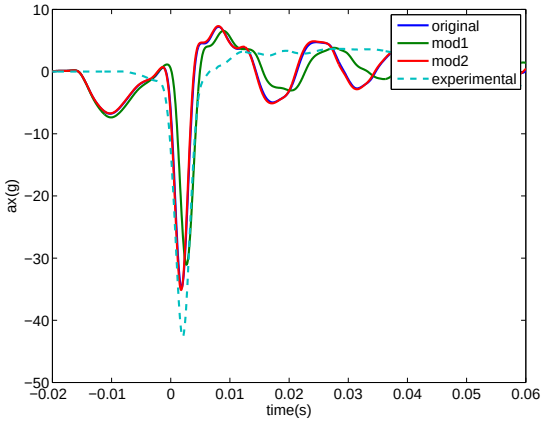

(o) Accelerations in x(g)

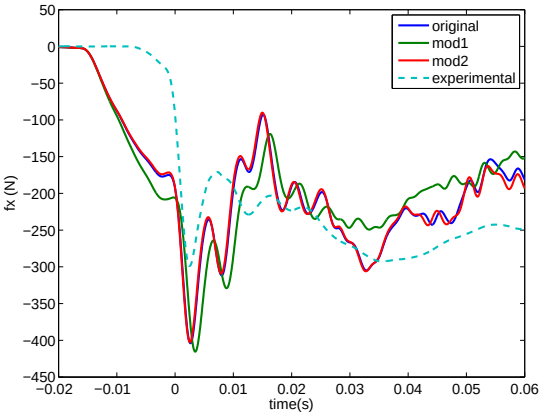

(p) Force in x(N)

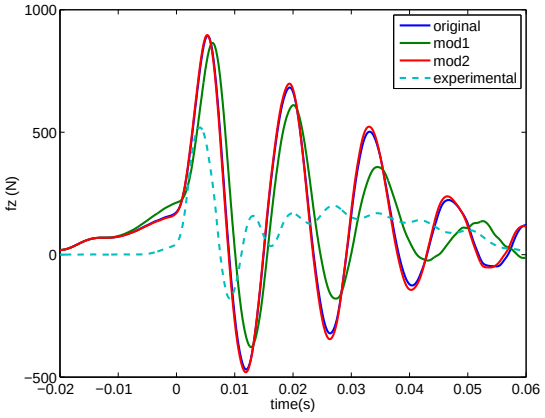

(q) Force in z(N)

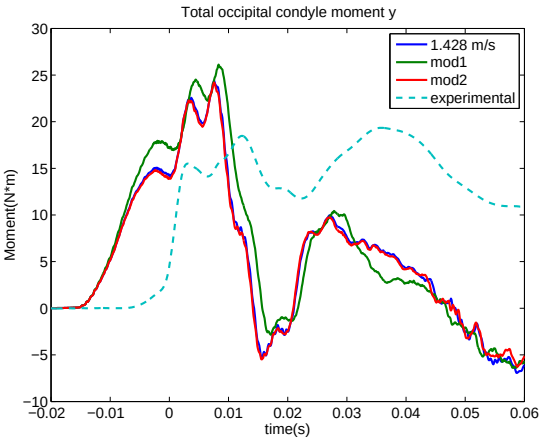

(r) Total Moment in y (N*m)

G(MPa)	a_x(g)	F_x(N)	F_z(N)	M_y(N·m)
6	-31.0699	-415.4995	864.1404	26.1227
0.6	-34.7715	-404.0127	893.6105	24.3701
0.06	-35.1487	-402.5776	896.5908	24.1917

Table 4.6: Maximum values of the variables

No changes respect the original results can be appreciated for low values of the infinite shear modulus. In the case of 6 MPa, it can be seen that the changes begin to be measurable, that is because the value of this parameter

starts to be relevant in the equation 4.2, affecting the value of the shear relaxation factor. This produces a variation on the acceleration and the rest of the magnitudes of interest (moments, forces...).

Skull material-1000002

It is the elastic material used for defining the skull part. Its behaviour is characterized by the density(ρ) and the Elastic Modulus (E). The first studied parameter was E, being the associated value of the green and red curve 7000 and $7 \cdot 10^5\ MPa$ respectively :

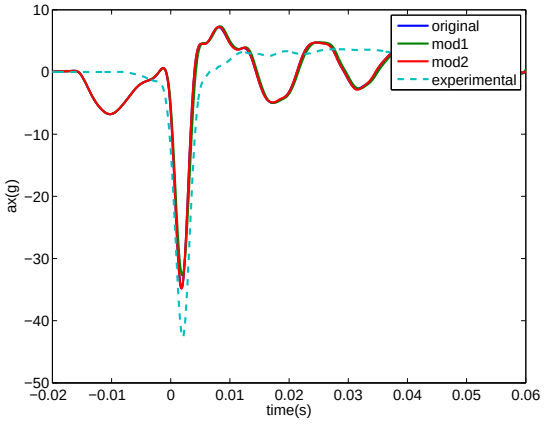

(s) Accelerations in x(g)

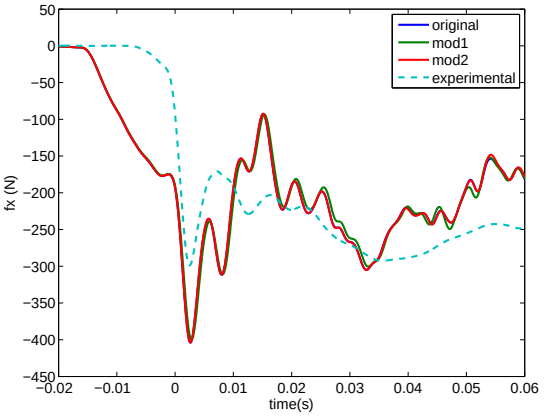

(t) Force in x(N)

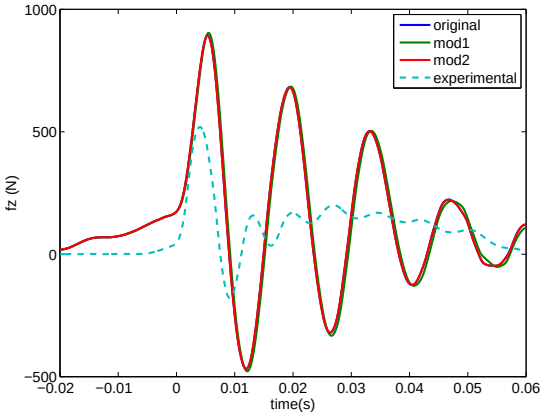

(u) Force in z(N)

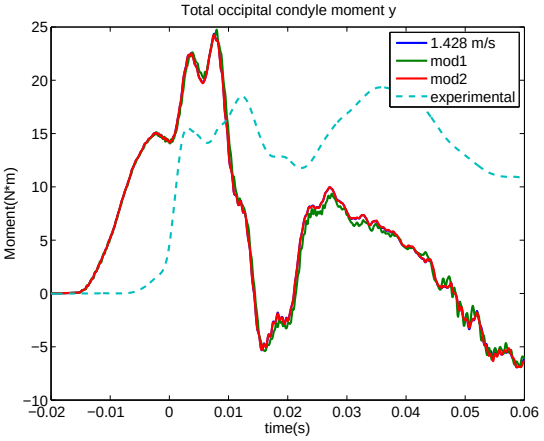

(v) Total Moment in y (N*m)

E(MPa)	a_x(g)	F_x(N)	F_z(N)	M_y(N·m)
7000	-32.7026	-399.9350	903.6337	24.7503
$7 \cdot 10^4$	-34.7715	-404.0127	893.6105	24.3701
$1 \cdot 10^5$	-34.8334	-403.7557	891.9428	24.2564

Table 4.7: Maximum values of the variables

There is nearly no difference for the results in the set of checked values. A small variation of the curve's maximum can be appreciated when the value of E is reduced, but it is not remarkable.

The other studied parameter was the density of the skull material. Small variations were also performed in order to observe the possible deviations that these modifications could cause in the results. The curves obtained were the following ones, being the green curve related to $2.2 \cdot 10^3 \ \frac{kg}{m^3}$ and the red one obtained using $3.2 \cdot 10^3 \ \frac{kg}{m^3}$:

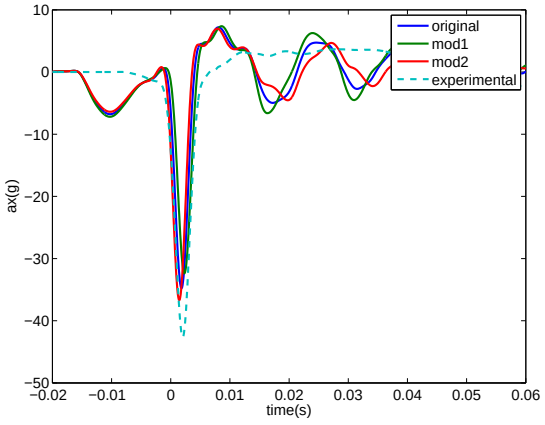

(w) Accelerations in x(g)

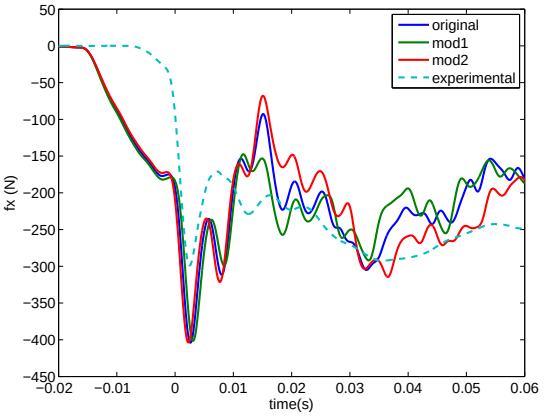

(x) Force in x(N)

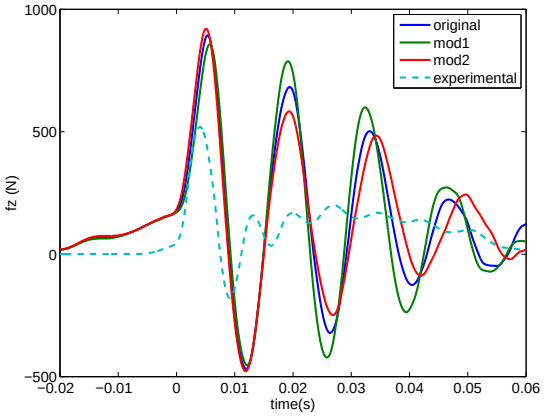

(y) Force in z(N)

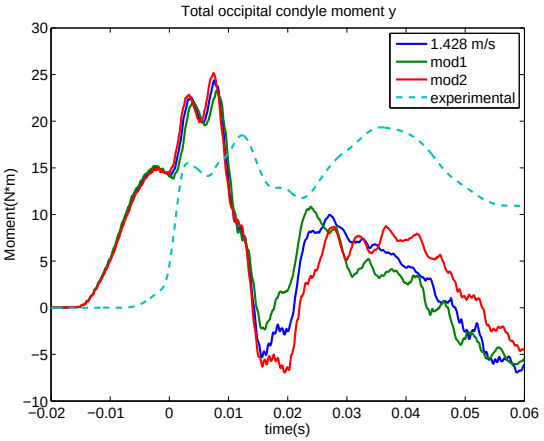

(z) Total Moment in y (N*m)

$\rho(\frac{kg}{m^3})$	a_x(g)	F_x(N)	F_z(N)	M_y(N·m)
$2.2 \cdot 10^3$	-32.3902	-401.5389	856.6362	23.2694
$2.7 \cdot 10^3$	-34.7715	-404.0127	893.6105	24.3701
$3.2 \cdot 10^3$	-36.7056	-403.6381	920.1775	25.1623

Table 4.8: Maximum values of the variables

It shows a similar tendency to the one observed for the same kind of variations in the skin material (1000000). As it has been explained, higher densities conduce to higher masses. This produces an increment of the inertial properties of the model that leads to an increase of the forces and moments generated in the head. These magnitudes are originated because a larger opposition of the neck is needed to stop the acceleration of the head, transmitted by the pendulum impact.

Neck rubber material-1000011

It was the viscoelastic material used for defining the part of the neck skin. Like the rest of the viscoelastic materials, it is defined by the infinite shear modulus(G_I), the short-time shear modulus (G_0), the bulk modulus (B), the

density (ρ) and the decay constant. The first checked variable was the bulk modulus, obtaining the following results:

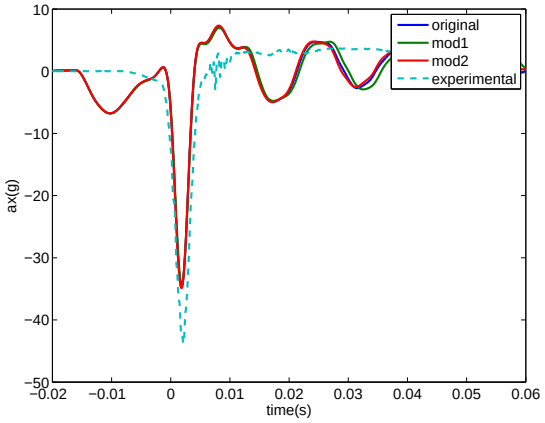

(aa) Accelerations in x(g)

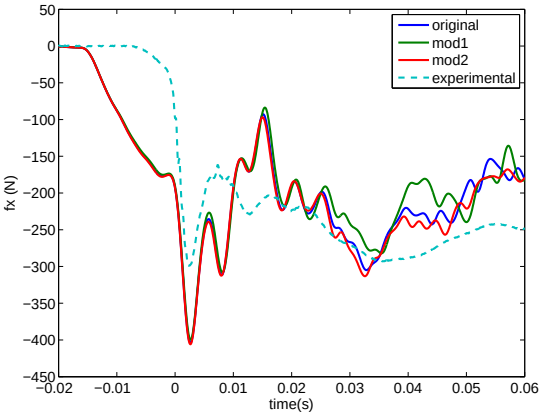

(ab) Force in x(N)

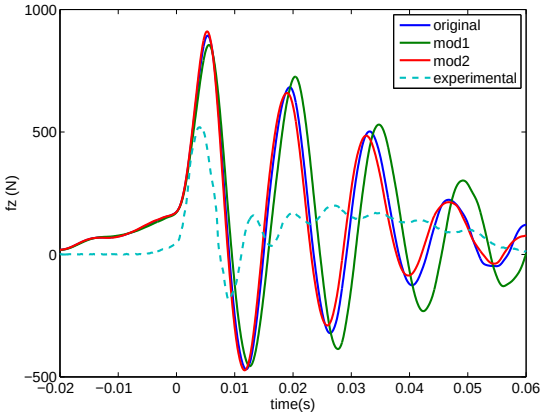

(ac) Force in z(N)

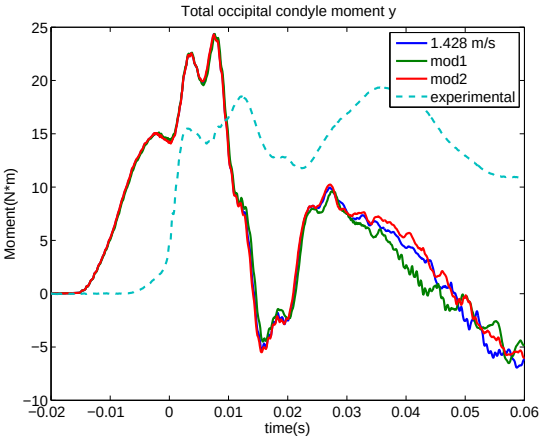

(ad) Total Moment in y (N*m)

$B(MPa)$	a_x(g)	F_x(N)	F_z(N)	M_y(N·m)
50	-34.3130	-399.6497	855.1264	24.3701
112.8	-34.7715	-404.0127	893.6105	24.3701
200	-34.8842	-405.9229	910.5231	25.3360

Table 4.9: Maximum values of the variables

The curves obtained for the different modifications are nearly identical, being nearly independent the results of the variables with respect to the variations of the bulk modulus. The only fact that can be remarked is that for low values of B, the maximum of the F_z is decreased but the time spent for damping the force becomes higher.

The next analysed parameter was the density. It was followed the same criteria stated before, obtaining the following results. The green curve is related to $2.2 \cdot 10^3 \ \frac{kg}{m^3}$ and the red one was obtained using $3.2 \cdot 10^3 \ \frac{kg}{m^3}$:

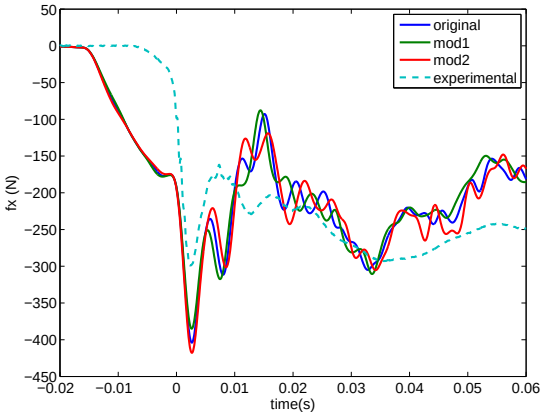

(ae) Force in x(N)

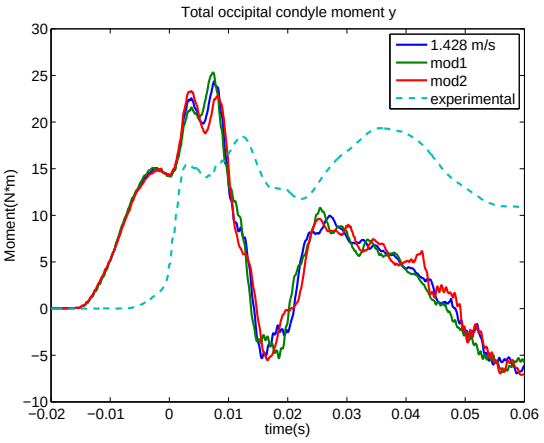

(af) Total Moment in y (N*m)

$\rho(\frac{kg}{m^3})$	a_x(g)	F_x(N)	F_z(N)	M_y(N·m)
$6.0 \cdot 10^2$	-34.7497	-384.9801	894.3677	25.3323
$1.1 \cdot 10^3$	-34.7715	-404.0127	893.6105	24.3701
$1.6 \cdot 10^3$	-34.5033	-417.9101	888.8302	23.3216

Table 4.10: Maximum values of the variables

In this case, no deviations have been observed for the frontal acceleration and vertical force so it has been decided not to attach them to the report as they do not provide any interesting result. In this case, it can be observed that the magnitudes have not responded in the same way that they did for

the density variation in the skull and the skin of the head. This is because the increment of the mass was produced on the neck this time, so it had no direct interaction with the force transmitted from the pendulum to the head (no difference in the frontal acceleration). The only possible variation that it could produce was an increment of the frontal force and moment suffered by the head, due to the increase of the opposition to the movement exerted by the neck if its density is increased. This is actually what it is observed.

The next studied material was the decay constant. In this case , two values were chosen to see their possible influence.The green curve is related to 1100 and the red one was obtained using 11. The resultant curves were the following ones:

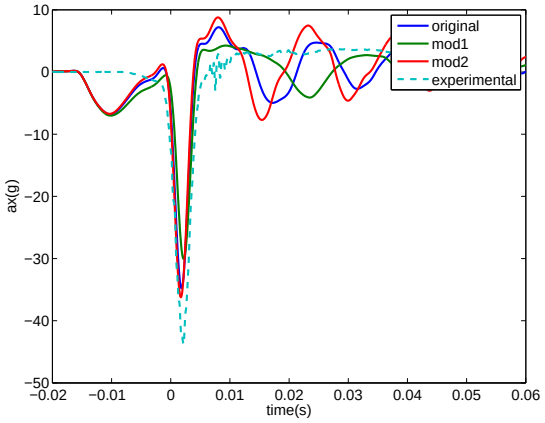

(ag) Accelerations in x(g)

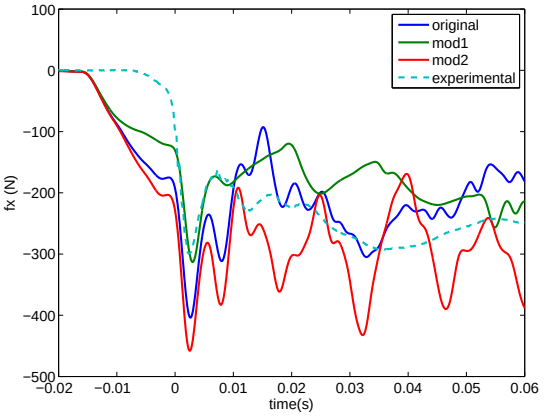

(ah) Force in x(N)

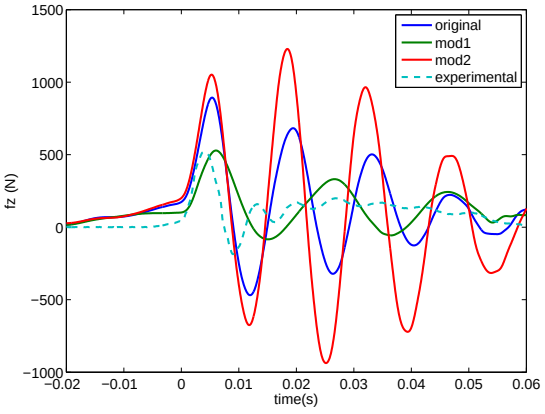

(ai) Force in z(N)

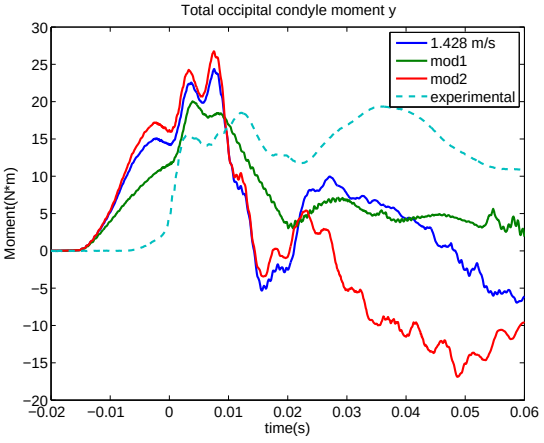

(aj) Total Moment in y (N*m)

$decay(1/s)$	a_x(g)	F_x(N)	F_z(N)	M_y(N·m)
1100	-30.0660	-313.1140	528.7077	20.0429
112.8	-34.7715	-404.0127	893.6105	24.3701
11	-36.2254	-458.0023	1229.1	26.7490

Table 4.11: Maximum values of the variables

It can be observed that this parameter has an important influence on the studied magnitudes. The results of the accelerations are not really affected by these modifications. For the moments and forces, it can be seen that for high values of β the maximum values of these variables decrease. Furthermore, the curve obtained for the frontal force F_x becomes smoother (more similar to the experimental one) and the vertical force F_z damps to the original value faster. It must be also remarked that the maximum values registered for the forces and moments are nearly identical to the ones obtained in the experimental results. This is because a higher decay constant originates a lower shear relaxation modulus according to the formula 4.2, producing a larger deformation of the rubber material if the stress applied remains constant. This increase of deformation in the neck allows to have a lower stress in the base of the head, decreasing the force and the moments suffered there.

The next studied parameter of the material was the short-time shear modulus G_0.The green curve is related to $46\ MPa$ and the red one was obtained using $0.46\ MPa$. The results achieved were the following ones:

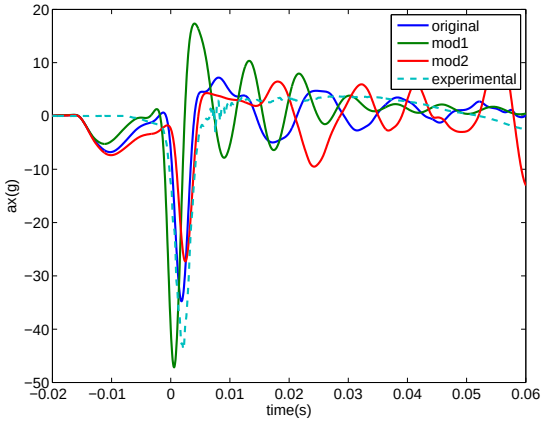

(ak) Accelerations in x(g)

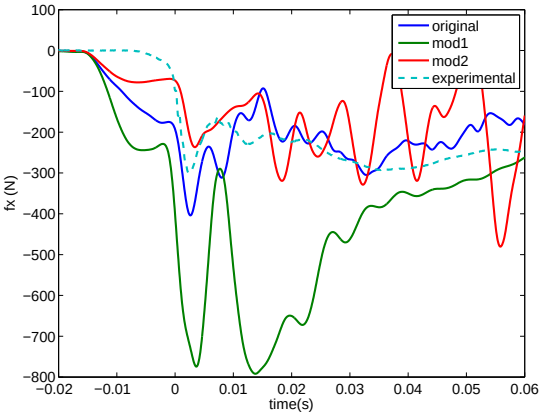

(al) Force in x(N)

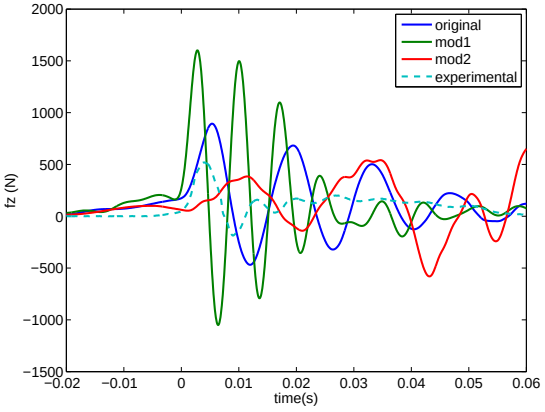

(am) Force in z(N)

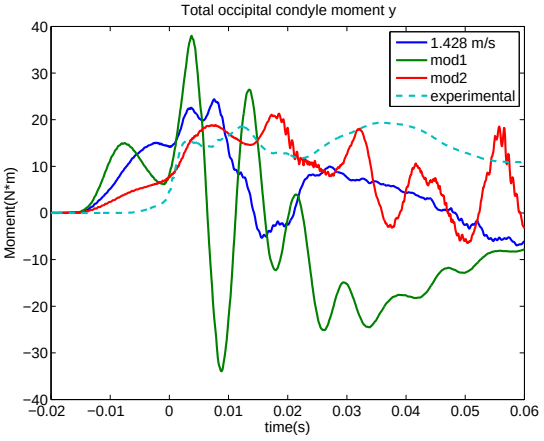

(an) Total Moment in y (N*m)

$G(MPa)$	a_x(g)	F_x(N)	F_z(N)	M_y(N·m)
46	-47.1696	-791.9231	1602	38.009
4.6	-34.7715	-404.0127	893.6105	24.3701
0.46	-27.2791	-577.3017	661.7582	19.3578

Table 4.12: Maximum values of the variables

In this case, it can be observed that when this parameter is drastically changed the behaviour becomes really unstable. This fact can be seen with the moments and forces. The vertical and frontal components achieve really

high peaks when this parameter goes to low values. Furthermore, the shape of the moment curve varies sensitively when this parameter is modified, achieving huge oscillations for high values of G_0.

The oscillations of the different variables decrease for low values of G_0. Recalling the equation 4.2, it can be deduced that decreasing this parameter will produce a similar effect to the one obtained increasing the decay constant.

Finally, a similar behaviour was observed in the sensitivity study of the infinite shear modulus G_∞. Its results are presented below, the green curve belongs to the case of 0.1 MPa while the red one is for 10 MPa:

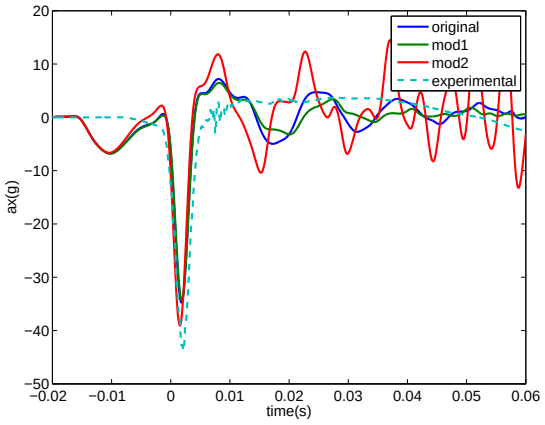

(ao) Accelerations in x(g)

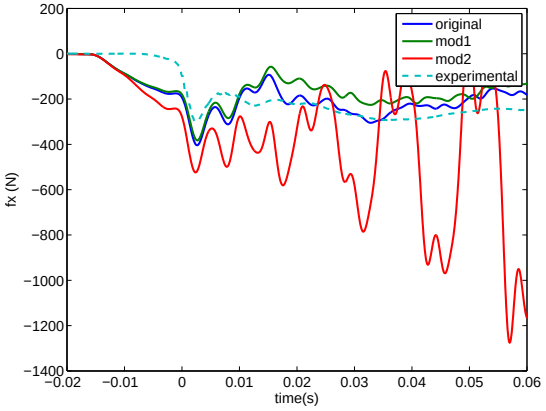

(ap) Force in x(N)

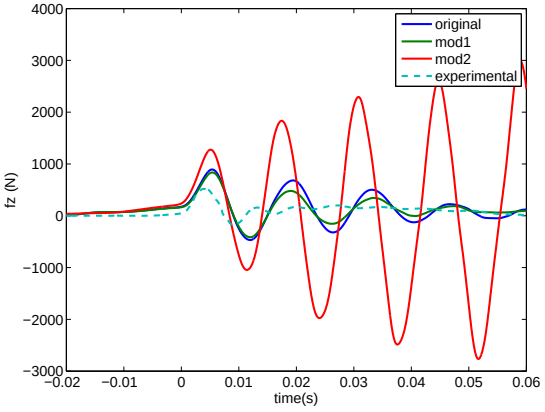

(aq) Force in z(N)

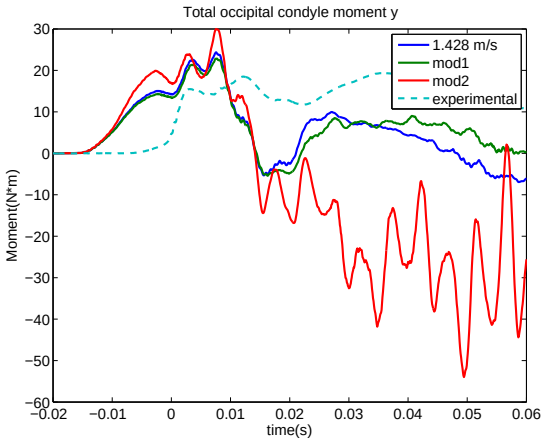

(ar) Total Moment in y (N*m)

$G(MPa)$	a_x(g)	F_x(N)	F_z(N)	M_y(N·m)
0.1	-34.2661	-382.4614	836.0859	22.8541
1	-34.7715	-404.0127	893.6105	24.3701
10	-39.0603	-1479.2	3010.2	-83.7475

Table 4.13: Maximum values of the variables

It can be deduced by the role that this parameter plays in the formula 4.2 that the results would be more unpredictable. For high values of G_∞ the results become really unstable, this manifests in the increasing vertical force F_z with time or the random values that the moment achieves. Therefore, this parameter should not be varied respect the original value.

Neck upper part-1000012

It was the material that defined the part of the neck involved in the joint between the neck and the head. In this case the elastic modulus E was the only parameter analysed. The results obtained were the following ones:

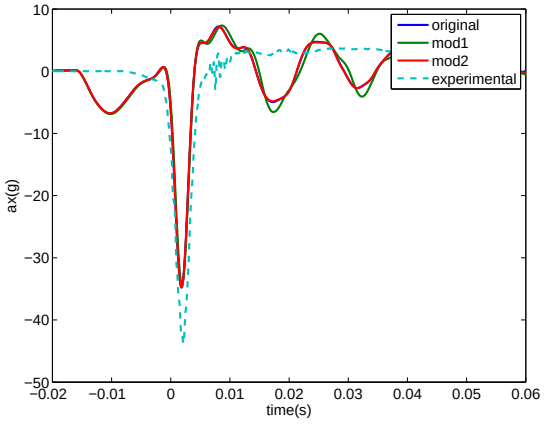

(as) Accelerations in x(g)

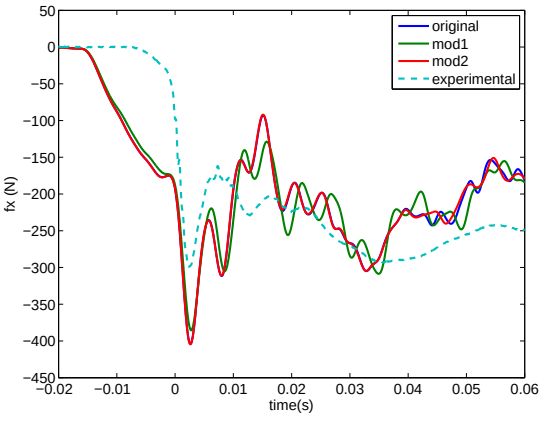

(at) Force in x(N)

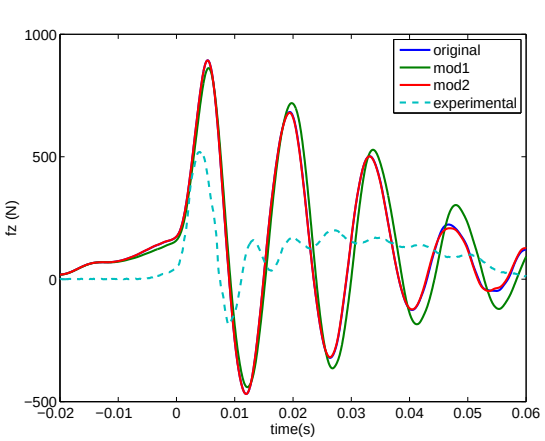

(au) Force in z(N)

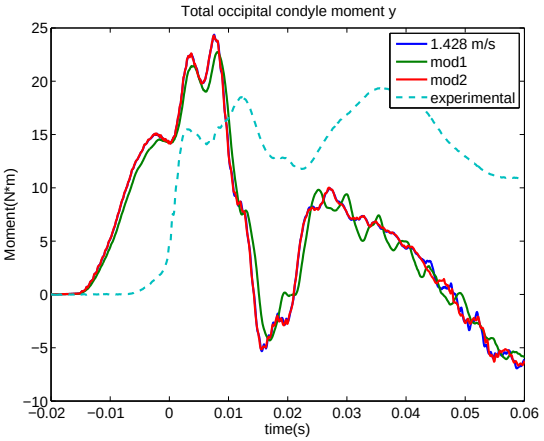

(av) Total Moment in y (N*m)

$E(MPa)$	a_x(g)	F_x(N)	F_z(N)	M_y(N·m)
7000	-34.2215	-385.4360	861.9202	22.7465
$7 \cdot 10^4$	-34.7715	-404.0127	893.6105	24.3701
$1 \cdot 10^5$	-34.7860	-404.5906	893.1341	24.2922

Table 4.14: Maximum values of the variables

It can be observed that the modifications do not provide any significant deviation in the results. The only observable difference is that the forces and moments become lower if the elastic modulus decreases.

Neck cable beam-1000018

It was the elastic material that defined the cable that went through the neck, giving stiffness to this part. In this case, the influence of the density (ρ) and the elastic modulus (E) were studied. Anyway, it will only be reported the results achieved for the elastic modulus because no variations were obtained for the modifications of the density. The green curve corresponds to the case of 80 MPa while the red one is related to 1000 MPa. The curves obtained were:

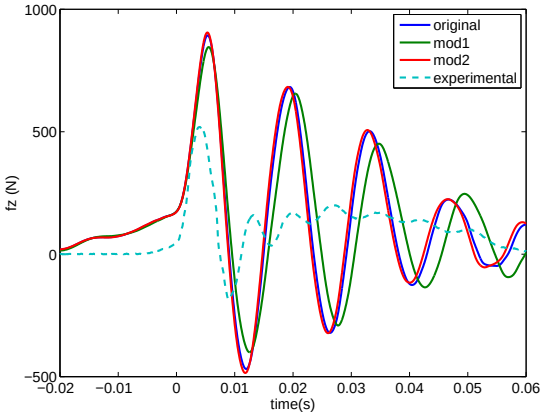

(aw) Force in z(N)

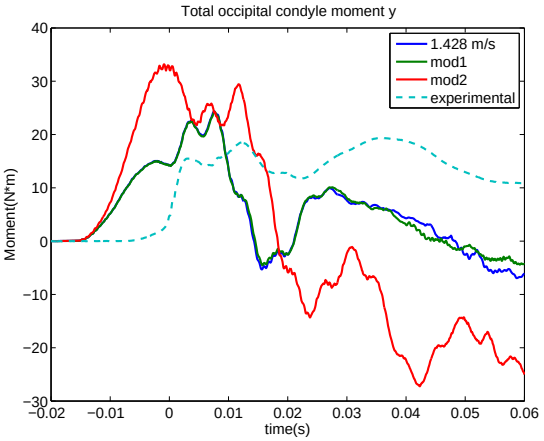

(ax) Total Moment in y (N*m)

$E(MPa)$	a_x(g)	F_x(N)	F_z(N)	M_y(N·m)
80	-34.5887	-402.3216	845.6110	24.3301
800	-34.7715	-404.0127	893.6105	24.3701
1000	-34.8207	-403.9674	905.0571	33.3578

Table 4.15: Maximum values of the variables

In this case, only the results of the vertical force F_z and the moment M_y have been attached because the rest remained invariant. It can be observed that if the Young Modulus is increased, the deformation that the neck will suffer will be lower. As the force applied remains constant, the resultant moment and force will be higher in the Occipital Condyle.

The materials that defined the joints (1000009,1000019,1000020,1000021), the neck disks (10000015) , null elements(1000022,1000010) and the base of the head(1000006) were also proved but no differences were appreciated.

4.1.2 Final tuning for pendulum impact

Finally, it has been tuned the values of the material parameters in order to reduce the differences between the simulations and the experimental behaviour. The parameters that mostly affected the results were the decay constants of the materials 1000000 and 1000011. By the results obtained, it has been decided to increase the values of the 1000000-material decay constant and 1000011-material decay constant to 2500 and 1100 respectively. The obtained results were the following ones:

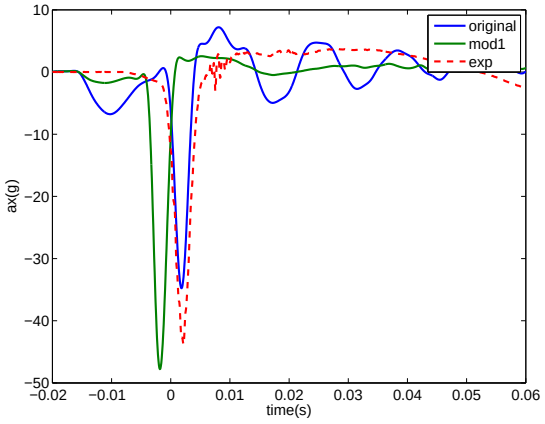

(ay) Accelerations in x(g)

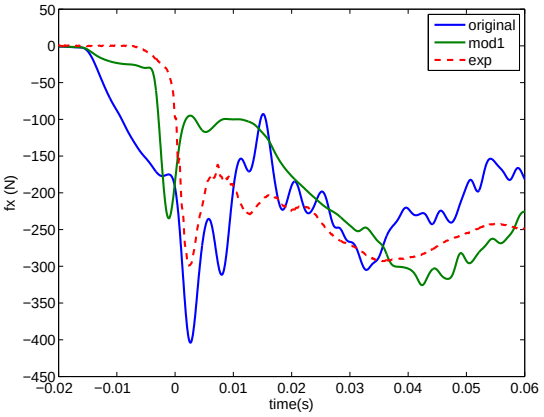

(az) Force in x(N)

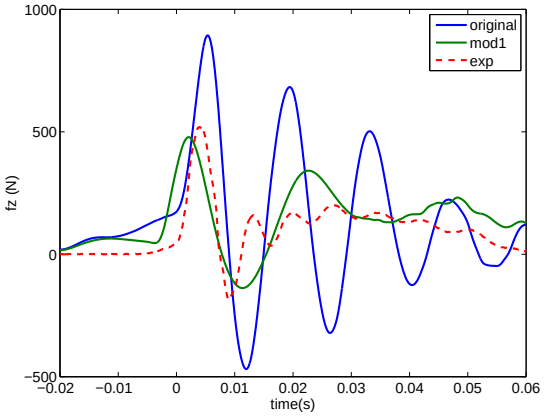

(ba) Force in z(N)

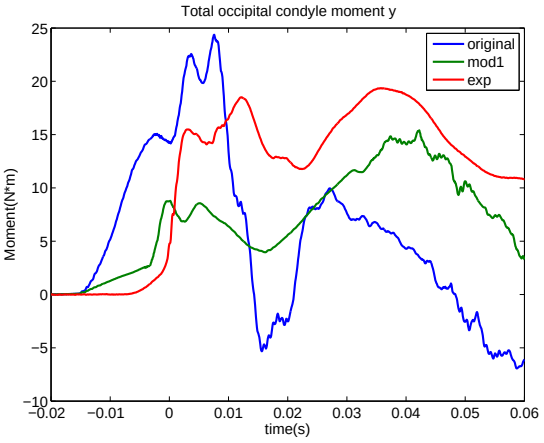

(bb) Total Moment in y (N*m)

simulations	a_x(g)	F_x(N)	F_z(N)	M_y(N·m)	HIC
original	-34.7715	-404.0127	893.6105	24.3701	11.9938
modified	-47.7891	-325.6715	478.0357	15.4084	23.7470
experiment	-43.8016	-298.8356	519.5586	19.3578	20.4745

Table 4.16: Maximum values of the variables

The results obtained with the modifications improve substantially the ones achieved with the original setting. First, the difference of the acceleration peaks decrease from 9.03 g to 3.9875 g , being the error 9.135%. Furthermore, the curve becomes smoother too, diminishing the peak originated by the nose deformation (which was not perceived by the experimental results). Regarding the frontal force, it can be seen that a similar behaviour happens, the shape of the curve becomes smoother and the difference between the maximums is reduced. For the frontal force, the maximum peak is nearly identical and the damping of the curve occurs much faster with this configuration. Finally, the moment curve achieves a more similar shape respect to the one obtained in the experiments.

The last studied criteria was the HIC, that shows more or less the mean acceleration distribution. It can be seen that the figure obtained for the modified simulation approximates closely to the value calculated in the experiments, being the error around a 16 %. It can be concluded that the modifications performed in the simulations have been effective for approaching the experiments.

4.2 Free fall

This simulation was basically prepared separating the head of the updated LSTC.NCAC_H3_50TH.130528_BETA model from the rest of the body and positioning it in the space in order to reproduce the conditions that characterized the free drop experiments. The upper part of the junction between the head and the neck was preserved for reproducing the presence of the neck transducer in the real experiment. For making the time spent for the simulation shorter, it was given an initial velocity to the head, which varied according to its supposed initial height . This made possible to position the head closer to the floor, being lower the time spent for having contact with this part and consequently the time spent for the computation. The velocities for each height were calculated using the conservation of energy between two different instants of time: at the initial instant of the drop and at 2 mm from the floor.

$$mgh_1 + \frac{1}{2}mu_1^2 = mgh_2 + \frac{1}{2}mu_2^2$$

Taking into account that the state 1 corresponded to the initial instant of time and 2 to the one at 2 mm it can be said that u_1 is 0. The different velocity solutions considering both heights (200 and 376 mm) were:

$$u_2 = \sqrt{2 * g * (h_1 - h_2)} = \sqrt{2 * g * (200 - 2)} = 1970.979mm/s \quad (4.3)$$

$$u_2 = \sqrt{2 * g * (h_1 - h_2)} = \sqrt{2 * g * (376 - 2)} = 2708.8521mm/s \quad (4.4)$$

After reporting the initial values that were used in the simulations, the default values for the different parameters of each material will be summarized in order to know the initial state of the model:

Material	ρ $(\frac{kg}{m^3})$	E(MPa)	G_0 (MPa)	$G_I(MPa)$	B(MPa)	decay$(\frac{1}{s})$
1000000	$1.2 \cdot 10^3$	-	30	0.6	25.6	250
1000001	$1.2 \cdot 10^3$	-	30	0.6	25.6	250
1000002	$2.7 \cdot 10^3$	$7.0 \cdot 10^4$	-	-	-	-
1000010	$1.0 \cdot 10^2$	50000	-	-	-	-

Table 4.17: Default values of the materials

Those materials were considered for the analysis because of the characteristics of the simulation. The experiment was an impact on the head so it can be intuitively predicted that the involved materials will be the ones used for defining its skin (1000000 and 1000001) and the skull (1000002 and 1000010). The rest of the materials defined the support elements (walls, ballasts, instruments) so they were not considered important.

The first fact investigated was the possible influence that the type of section of the floor could have on the results. For this reason two possible sections for the floor were considered: shell elements and a rigid floor. The curves obtained are the following ones:

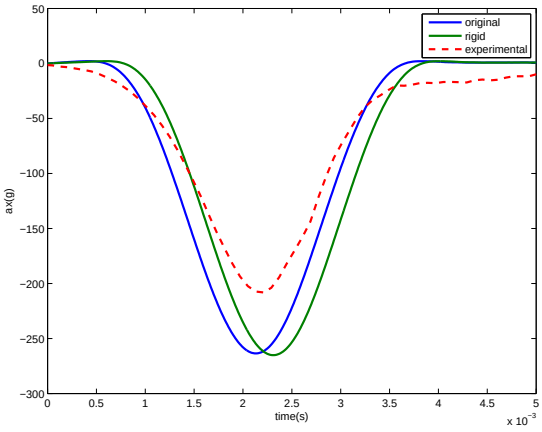

(bc) Accelerations in x(g)

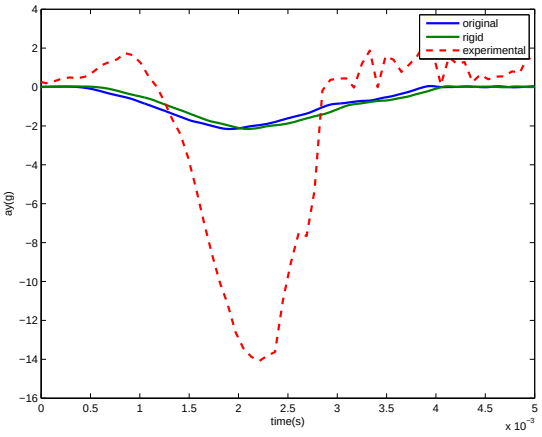

(bd) Accelerations in y(g)

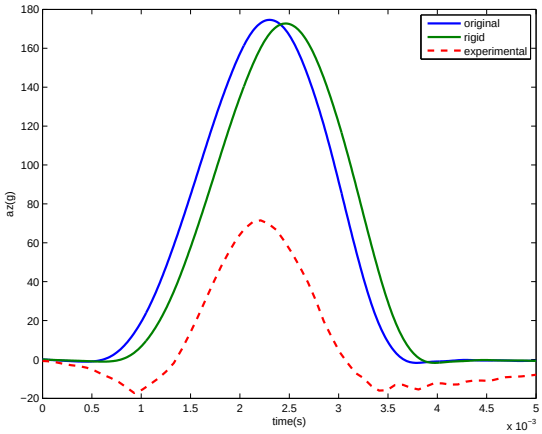

(be) Accelerations in z(g)

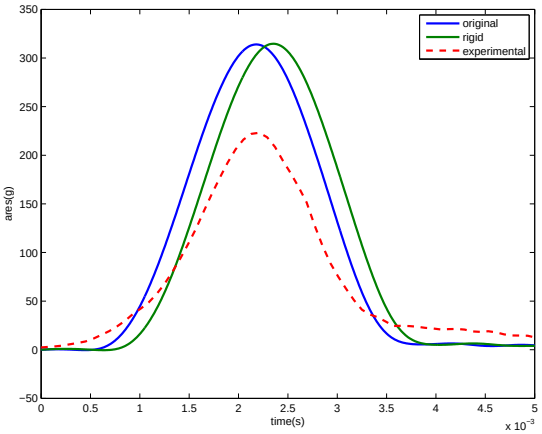

(bf) Resultant acceleration(g)

From a qualitative point of view, it can be observed that there are no measured accelerations until the head impacts on the floor. After that, the acceleration peak starts to increase once the contact is produced, being its maximum the instant of time when the head is totally stopped by the action of the wall. Finally, the head rebounds, returning the accelerations to their initial zero-value state. It could be important to recall that the accelerations were measured respect a system of reference placed inside the head so the originated values were produced by the action of an external factor affecting the relative position of the head elements (the impact of the wall in this case).

From the numerical point of view, it can be seen that there is nearly no difference between the maximum values obtained for the rigid wall and those ones calculated with the shell elements. The exact values will be attached now:

Accelerations	$a_x(g)$	$a_y(g)$	$a_z(g)$	$a_{res}(g)$
original	-263.5452	-2.1575	174.6183	313.9631
rigid	-265.1282	-2.1557	172.7454	314.6538
experimental	-208.1165	-14.0849	71.5233	223.1289

Table 4.18: Maximum values of the accelerations

As it can be seen, there is an important difference between the acceleration peaks of the simulations and those ones obtained in the experiment, achieving a 30% of variation for the resultant parameter. The difference becomes huge for the case of the lateral acceleration but it won't be taken into account because it improves the results obtained in the experiments (the desired behaviour was to minimize this value). It can also be observed that the differences between the simulation and the experimental peaks are a little bit lower for the case of the shell elements so, even if it is not the most efficient solution in terms of computational cost, it was decided to use the original option because it slightly improves the results and the additional time required for this configuration is still affordable.

4.2.1 Sensitivity analysis

After obtaining the results of the original configuration, another sensitivity analysis was performed to look for a more realistic behaviour. In this study, it was observed that the general tendencies seen in the last section were not valid because the way of transmitting the force to the head was different. In the last simulation,it was produced a negative displacement in the relative X axis of the S.R. in the head. In this case, the direction of the motion is not totally aligned with the position of X axis in the head's S.R. so the direction of the applied force was not exactly equal in both simulations . Additionally, it was the head the one that moved towards the wall in this case (having a positive relative displacement from this S.R. point of view). For these reasons, the expected behaviours will change totally from the ones obtained before.

Skin material-1000000

This material was the one used for the skin of the front of the head. It was a viscoelatic material so, as it has been stated before, its behaviour was characterized by the infinite shear modulus(G_I), the short-time shear modulus

(G_0), the bulk modulus (B), the density (ρ) and the decay constant. The first studied variable was the bulk modulus, obtaining the following results:

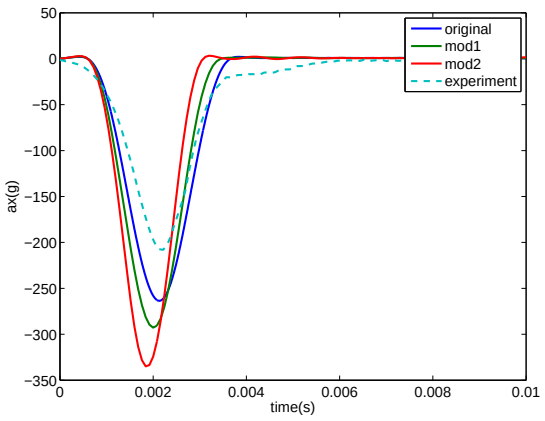

(bg) Accelerations in x(g)

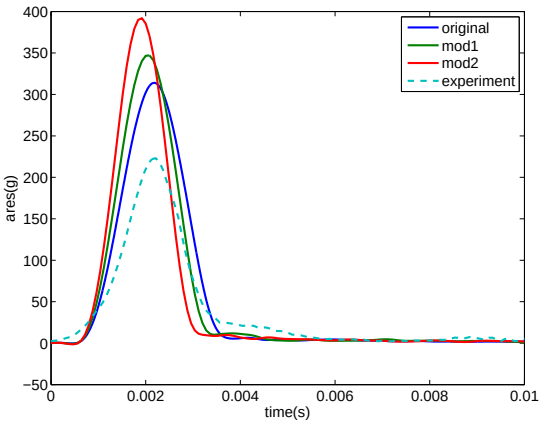

(bh) Resultant acceleration(g)

B(MPa)	a_x(g)	a_{res}(g)
25.6	-263.5452	313.9631
50	-292.8036	347.0743
100	-334.9041	391.9285

Table 4.19: Maximum values of the accelerations for each value of B

It can be observed that if the bulk modulus of this material increase, the frontal and resultant acceleration peaks registered also do it. Anyway, the relation between the value of a_{res} and the bulk modulus is non linear. The values that were tested are in both cases higher than the default one (Table 4.1) because it can not be proved a value for the Bulk modulus lower than $\frac{2}{3}$ of G_0 so the default value was already on the limit.

After that, the variation of the density(ρ) was checked. The green curve corresponded to $7.0 \cdot 10^2$ and the red one to $1.7 \cdot 10^3$. In this case the different densities varied only in a small percentage because if the changes were considerable, the resultant material would not be realistic,being its results worthless.

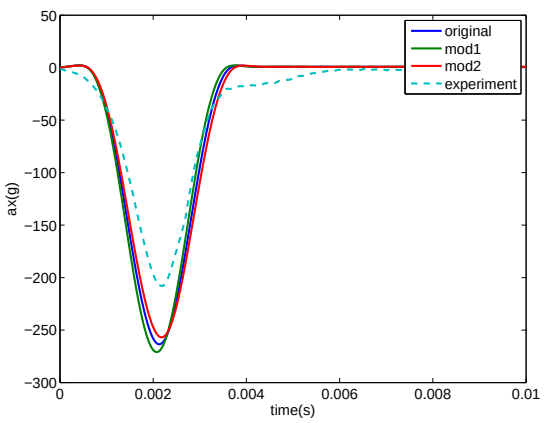

(bi) Accelerations in x(g)

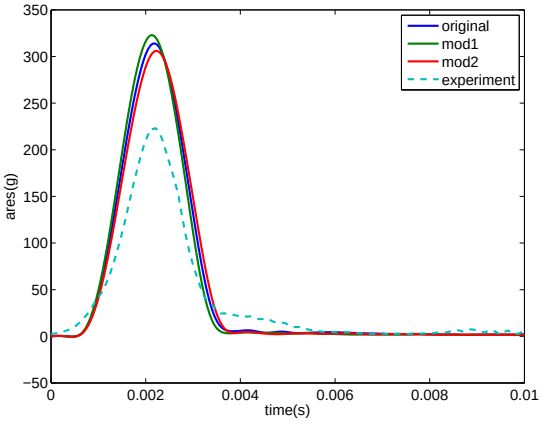

(bj) Resultant acceleration(g)

$\rho(\frac{kg}{m^3})$	a_x(g)	a_{res}(g)
$7.0 \cdot 10^2$	-270.9773	322.9
$1.2 \cdot 10^3$	-263.5452	313.9631
$1.7 \cdot 10^3$	-256.9147	305.9644

Table 4.20: Maximum values of the accelerations for each value of ρ

As it can be seen, the variations on the density do not affect considerably the results of the accelerations. Anyway, it can be observed that if the density increases, the frontal and resultant accelerations decrease, happening in the other way if it decreases. This is due to the fact that a higher density increases the force necessary to provide the same displacement than before, if the force remains constant the deformation of the skin part will be lower and consequently the acceleration that the instrumentation cube suffers will decrease. To have a better understanding of this concept it can be recalled the Second Newton Law. If the mass increases (higher density) and the force remains constant (drop from a certain height) the acceleration will be lower.

After that, the influence of the decay constant was studied. The green curve corresponded to 2500 and the red one to 25. In this case the variations

proved were quite important because it was a critical term, as it has been explained in the last section:

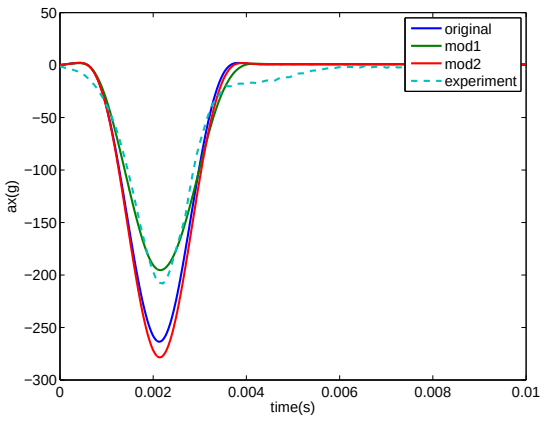

(bk) Accelerations in x(g)

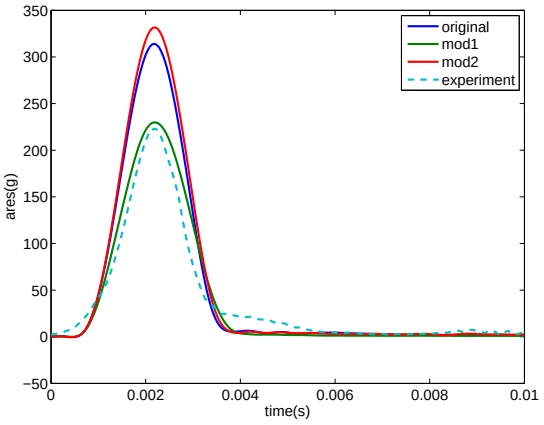

(bl) Resultant acceleration(g)

decay($\frac{1}{s}$)	a_x(g)	a_{res}(g)
2500	-195.3518	229.8189
250	-263.5452	313.9631
25	-278.4460	331.1289

Table 4.21: Maximum values of the accelerations for each value of decay constant

In this case, it has been found that the variations on the decay constant modify sensitively the acceleration peaks. This is because for the viscoelastic materials the shear relaxation behaviour is modeled with the following formula, as it has been said in the last section:

$$G(t) = G_\infty + (G_0 - G_\infty)\exp -\beta t \tag{4.5}$$

The decay constant has an exponential relation inside the shear relaxation formula so that is the reason why the variation of this constant produced those differences. If the decay constant is increased, the relaxation shear modulus obtained will be lower and consequently the internal stress generated will

decrease too.

$$\sigma_{ij} = 2\int_0^t G(t-\tau)D_{ij}d\tau \tag{4.6}$$

Being D_{ij} the strain rate matrix. This will generate lower internal displacements and the accelerations will be lower, consequently.

Then, the influence of the infinite shear stress G_I was studied on the simulations. The green curve corresponded to $0.06\ MPa$ and the red one to $6\ MPa$.

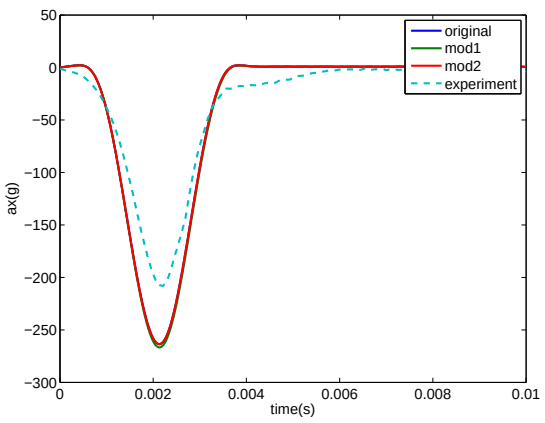

(bm) Accelerations in x(g)

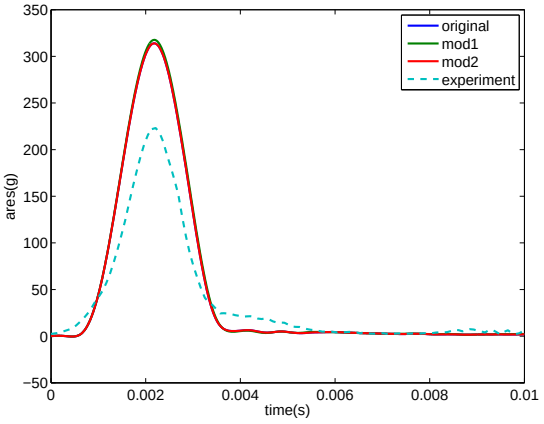

(bn) Resultant acceleration(g)

G_I(MPa)	a_x(g)	a_{res}(g)
0.06	-263.5424	313.9605
0.6	-263.5452	313.9631
6	-266.6413	317.6630

Table 4.22: Maximum values of the accelerations for each value of infinite shear

It nearly has no influence over the resultant accelerations because its relation is linear with respect the shear relaxation formula 4.5 so the differences

produced on $G(t)$ will be really small. Anyway, it was considered for observing if its influence could have changed respect the results obtained in the last section. As it does not provide much information, no additional results related with this parameter will be attached in the work.

Finally, it was analysed the influence of the short-time shear modulus. Only one value of this paramater could be analysed because of the existent relation with the bulk modulus, as it has been explained before:

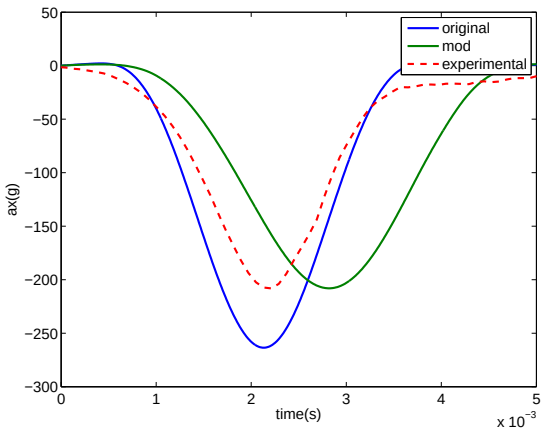

(bo) Accelerations in x(g)

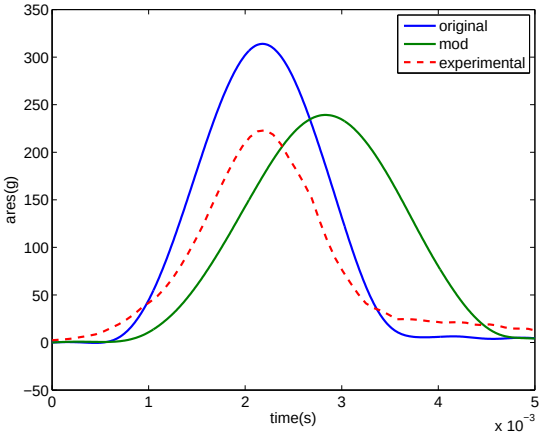

(bp) Resultant acceleration(g)

G_0(MPa)	a_x(g)	a_{res}(g)
3	-208.0462	239.2171
30	-263.5452	313.9631

Table 4.23: Maximum values of the accelerations for each value of short-time shear modulus

By these results, it can de deduced that decreasing G_0 produces a similar effect than increasing the decay constant. Recalling the formula 4.5, the resultant shear relaxation modulus becomes lower so the stress generated will be lower, producing a lower displacement and resultant acceleration. Furthermore, it can also be highlighted that the checked value of G_0 nearly give a

maximum acceleration peak in the X axis that corresponds to the experimental one. Anyway, it also produces a delay in the rising of the corresponding peaks.

Skull material-1000002

In this case, the material of the head was analysed. It was an elastic material so the main checked properties were the density (ρ) and the Young modulus(E). The first studied parameter was the Young Modulus:

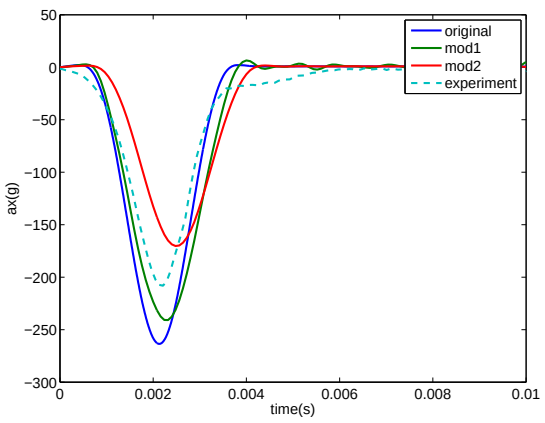

(bq) Accelerations in x(g)

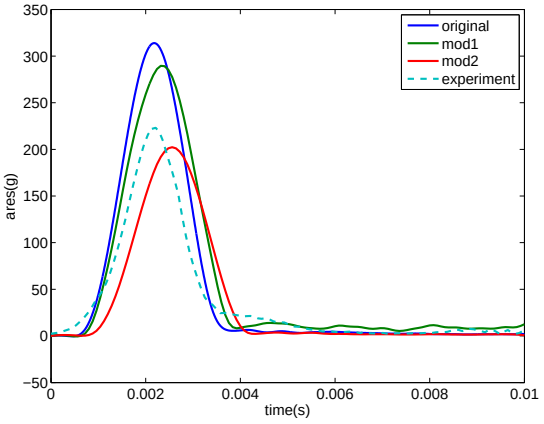

(br) Resultant acceleration(g)

E(MPa)	a_x(g)	a_{res}(g)
$7 \cdot 10^{-3}$	-240.8750	289.5405
$7 \cdot 10^{-4}$	-263.5452	313.9631
$1 \cdot 10^{-5}$	-170.3078	202.3439

Table 4.24: Maximum values of the accelerations for each value of the Young Modulus

It can be observed that the behaviour of this material is more random because the peak of the accelerations decrease for both values proved. It is an hypoelastic isotropic material, which means that its stress won't be a linear function of the strain. In isotropic materials, G can be related to the elastic

modulus E by means of the formula:

$$2G(v+1) = E \tag{4.7}$$

where v is the Poisson's ratio. It can be observed that the variations over the Young modulus affect directly over the stress generated and consequently over the strain too, producing changes in the acceleration.

Finally, the possible influence of the density on the results was also analysed. In this case, a variation of $\pm 0.5 \cdot 10^3 \ \frac{kg}{m^3}$ was applied to the default value to obtain the different curves:

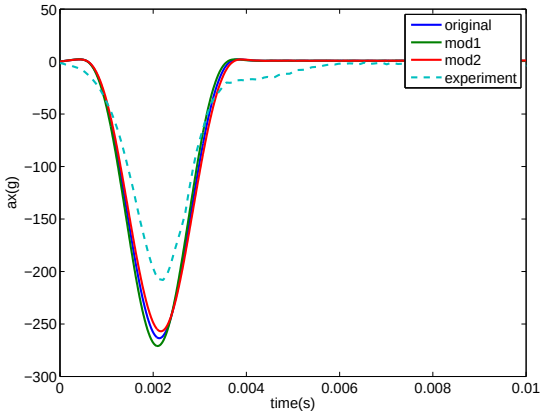

(bs) Accelerations in x(g)

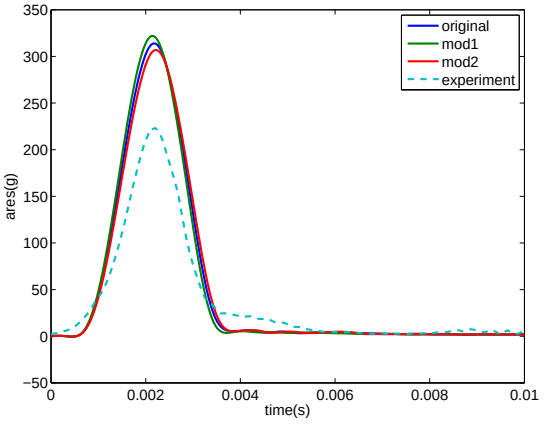

(bt) Resultant acceleration(g)

$\rho(\frac{kg}{m^3})$	a_x(g)	a_{res}(g)
$2.2 \cdot 10^3$	-270.9906	321.9650
$2.7 \cdot 10^3$	-263.5452	313.9631
$3.2 \cdot 10^3$	-256.9486	306.8302

Table 4.25: Maximum values of the accelerations for each value of the densities

The results slightly change for the different values of the density. Anyway, the acceleration peaks decrease for higher densities because the force applied

to the head was constant for all the cases (impact from a certain height), as it has been stated previously.

Head material-1000010

In this case it is a null material. This kind of materials prevent the solid elements to become too compressed. By means of this material, a contact is stablished between the shell elements of the model. Young modulus (E) and Poisson's ratio are only used for modelling the contact interface stiffness but their values must be accurate. In this case, the Young modulus was varied to see its influence:

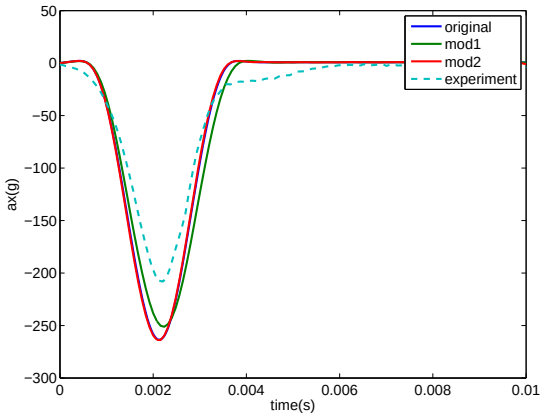

(bu) Accelerations in x(g)

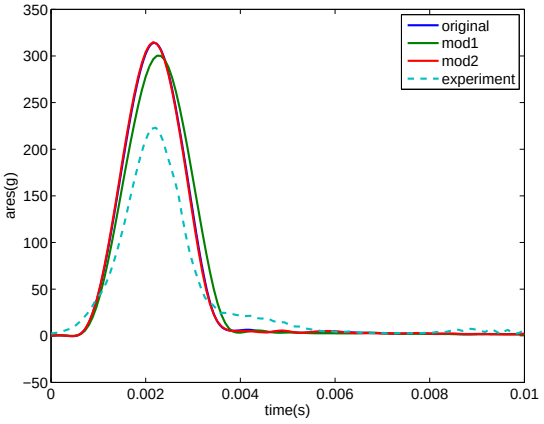

(bv) Resultant acceleration(g)

YM(MPa)	a_x(g)	a_{res}(g)
$5 \cdot 10^3$	-251.1889	300.2962
$5 \cdot 10^4$	-263.5452	313.9631
$5 \cdot 10^5$	-263.7896	314.8110

Table 4.26: Maximum values of the accelerations for each value of the Young Modulus

There is nearly no difference between the studied values. The only variation

that can be observed is that the acceleration peaks decrease for decreasing values of the Young Modulus.

A sensitivity analysis was also performed for the material that define the rear part of the head (1000001) but the results obtained were exactly equal for all the cases so its influence was neglected.

4.2.2 Final tuning for free fall results

It can be observed that the most relevant parameter for this kind of simulations have been the decay constant of the material 1000000. For this reason, it was decided to find the correct tuning of this parameter to obtain the same behaviour in the simulations and in the experiments. By an iterative process, it has been obtained that a decay constant of 2600 give quite good results. The figures obtained for the case of 376, where the nose is higher than the front of the head, are:

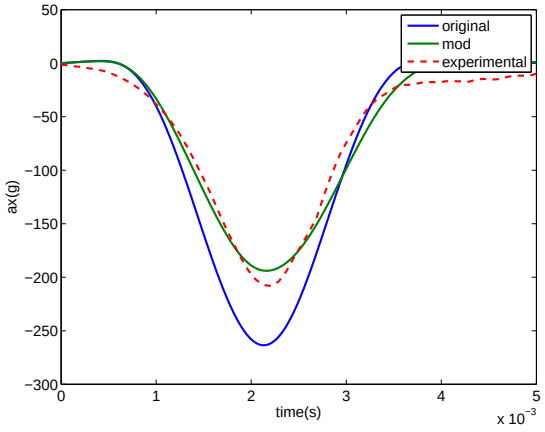

(bw) Accelerations in x(g)

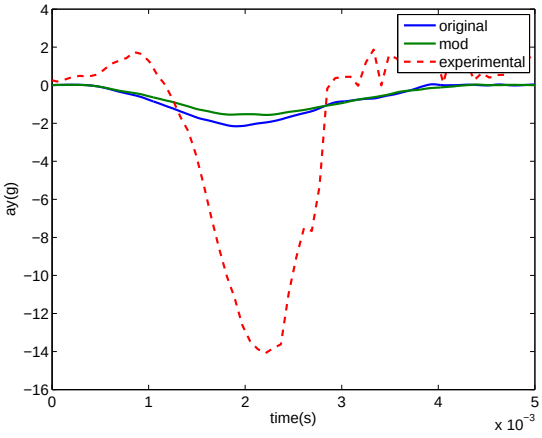

(bx) Accelerations in y(g)

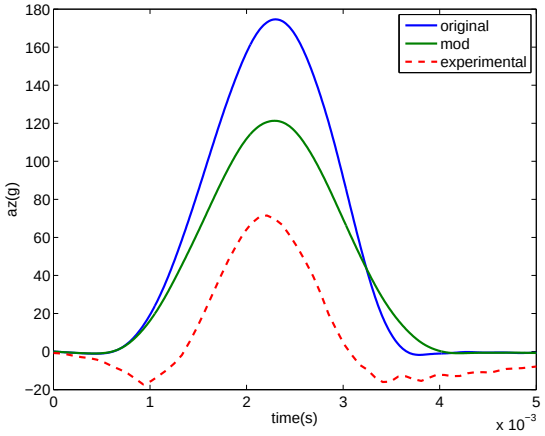

(by) Accelerations in z(g)

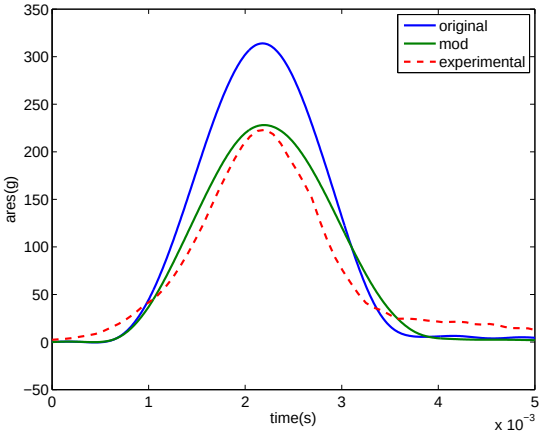

(bz) Resultant accelerations(g)

simulation	a_x(g)	a_{res}(g)
mod	-193.9651	223.1289
original	-263.5452	313.9631
experimental	-208.1165	228.0882

Table 4.27: Maximum values of the accelerations for each case of 376-

The results obtained are nearly perfect for the cases of the resultant acceleration and its x component in terms of the peak achieved, being 6.8 % the maximum error obtained. Furthermore, the difference was also decreased for the case of the Z axis. This modification was also checked with the experimental results obtained for the cases of 200 mm and 376 mm with nose lower than the front of the head:

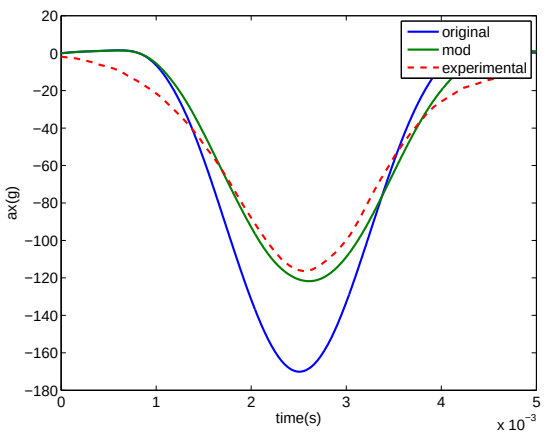

(ca) Accelerations in x(g)

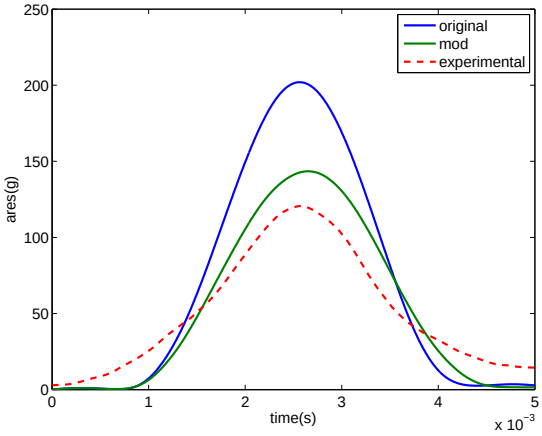

(cb) Resultant acceleration(g)

simulation	a_x(g)	a_{res}(g)
mod	-121.7470	143.4421
original	-170.0832	201.9719
experimental	-116.4350	120.6123

Table 4.28: Maximum values of the accelerations for each case of 200

For the case of 200 mm, it can be observed that in the X axis the correlation is nearly pefect while the resultant acceleration has an error of 18.928%. Anyway, this increment of the error is due to the fact that the experiments were not perfect so there will always exist deviations in the errors between the different configurations. Finally, it was checked the results for the last configuration:

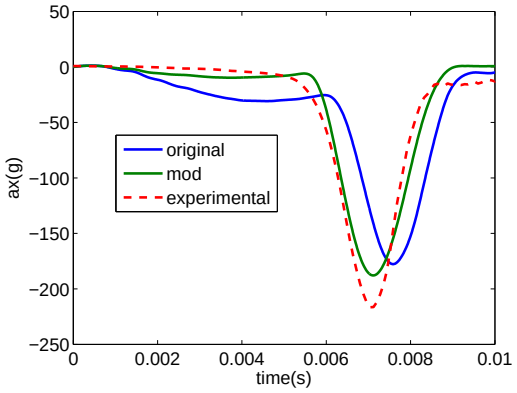

(cc) Accelerations in x(g)

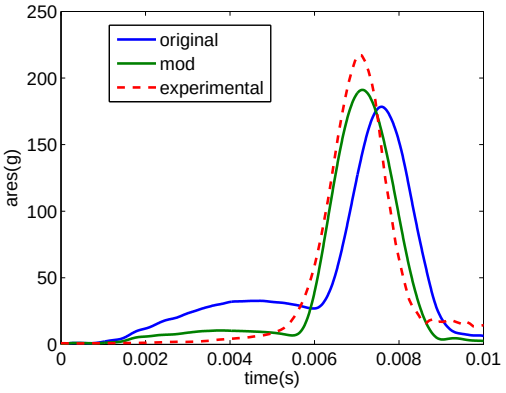

(cd) Resultant acceleration(g)

simulation	a_x(g)	a_{res}(g)
mod	-187.8970	191.1043
original	-177.6803	178.4151
experimental	-216.5159	217.2021

Table 4.29: Maximum values of the accelerations for each case of 376+

In this case it can also be observed that the deviation between the peaks was also reduced and their amplitude is nearly identical with respect the results obtained in the experiments. For these reasons, it can be considered that the modification performed for the simulations is valid to reproduce the real behaviour.

Chapter 5

Conclusions and further developments

The present work was focused on improving the results of the simulations to obtain a more realistic behaviour. The first part of the work was related to the adquisition of experimental data for comparing them with the curves obtained in the simulations. Regarding the data collected from the impact of the pendulum on the head , no further comments can be done because it was performed for the development of another thesis. Nevertheless, the head drop test showed some interesting facts.

The results obtained were characterized by a really high dispersion among the experiments with the same configuration. This proves that it is necesary to perform more tests in order to see if the dispersion is reduced and the results become more exact. Furthermore, the method for positioning the head in the space should be improved because it could be an important factor that may influentiate the results.

From the numerical part, it can be said that the most important parts of the model in the simulation, the ones that recreated the response of the head after the impact of the pendulum, were the expected ones: skull, skin of the head, cable through the neck and the neck itself. In the case of the

head drop, the main parts were the skull and the skin of the head. It can be deduced that the skin of the head plays an important role in its response to an external force. Most of the energy is absorbed in this part so a correct tuning of the paramaters that define this material is important to reproduce the real behaviour. Furthermore, the viscoelastic material of the neck contributes deeply in the behaviour of the head too, being the most important factor for regulating the moment and force response at the Occipital Condyle. Among all the studied parameters that define the different materials, it can be concluded that the decay constant is the most important one, being its correct tuning vital for obtaining a realistic behaviour of the model.

Regarding the results of the final tuning of the parameters performed in both simulations, it can be seen that the differences between the curves of the simulations and the experimental ones were diminished drastically. Despite of this, they were obtained by the modification of one type of parameter (decay constant) so they can be improved including the influence of the other ones. This refining of the results was not performed due to the lack of time but it can be faced in future researches.

Bibliography

[1] Arosio, Benedetta., *Anthropomorphic test device and total human model head ande neck injury analysis based on experimental and numerical activity*

[2] S. Jones, Ian, *Calibration Review and Head Impact Analysis of a Hybrid III dummy*

[3] G.McHenry , Brian, *Head Injury Criterion and the ATB*

[4] *Dummy performance and test procedure*

[5] *Crash Analysis Criteria Description* Arbeitskreis Messdatenverarbeitung Fahrzeugsicherheit

[6] Guha,Sarba, *LSTC Hybrid III dummies Positioning and Post-Processing*

[7] SAE International, *SAE j211-1:instrumentation for impact testing*

[8] K.Jarett,M.Saloum,B.Wade,C.Morgan,S.Moss and Y.Zhao, *Hybrid III Dummy Family Update- 10 year old and Large male*

[9] John O. Hallquist, *LS-Dyna Theory manual*